Journal of
Iberian Geology
AN INTERNATIONAL PUBLICATION OF EARTH SCIENCES

Revisiting the Late Jurassic-Early Cretaceous of the NW South Iberian Basin: new ages and sedimentary environments

S. Campos-Soto[1,2]*, M. I. Benito[1,2], R. Mas[1,2], E. Caus[3], A. Cobos[4], P. Suarez-Gonzalez[1,2], I. E. Quijada[5]

[1]*Departamento de Estratigrafía, Facultad de Ciencias Geológicas, Universidad Complutense de Madrid, 28040 Madrid, Spain*
[2]*Instituto de Geociencias IGEO (CSIC, UCM), C/ José Antonio Novais 12, 28040 Madrid, Spain*
[3]*Departament de Geologia (Unitat de Paleontologia), Universitat Autònoma de Barcelona, 08193 Cerdanyola del Vallés, Spain.*
[4]*Fundación Conjunto Paleontológico de Teruel-Dinópolis, Avda. Sagunto, 44002 Teruel, Spain*
[5]*Departamento de Geología, Universidad de Oviedo, C/Jesús Arias de Velasco s/n, 33005 Oviedo, Spain.*

e-mail addresses: sonia.campos.soto@ucm.es (S.C-S. Corresponding author); mibenito@ucm.es (M.I.B.); ramonmas@ucm.es (R.M.); esmeralda.caus@uab.es (E.C.); cobos@dinopolis.com (A.C.); pablosuarez@ucm.es (P.S-G.); emma@geol.uniovi.es (I.E.Q.)*

Abstract

The study of the Upper Jurassic-Lower Cretaceous deposits (Higueruelas, Villar del Arzobispo and Aldea de Cortés Formations) of the South Iberian Basin (NW Valencia, Spain) reveals new stratigraphic and sedimentological data, which have significant implications on the stratigraphic framework, depositional environments and age of these units. Moreover, these new data encourage revising the previously proposed stratigraphic correlations between the studied units and those deposited in adjacent areas of the Iberian Basin.

The Higueruelas Fm was deposited in a mid-inner carbonate platform where oncolitic bars migrated by the action of storms and where oncoid production progressively decreased towards the uppermost part of the unit. The overlying Villar del Arzobispo Fm has been traditionally interpreted as an inner platform-lagoon evolving into a tidal-flat. Here it is interpreted as an inner-carbonate platform affected by storms, where oolitic shoals protected a lagoon, which had siliciclastic inputs from the continent. The Aldea de Cortés Fm has been previously interpreted as a lagoon surrounded by tidal-flats and fluvial-deltaic plains. Here it is reinterpreted as a coastal wetland where siliciclastic muddy deposits interacted with shallow fresh to marine water bodies, aeolian dunes and continental siliciclastic inputs.

The contact between the Higueruelas and Villar del Arzobispo Fms, classically defined as gradual, is interpreted here as gradual and rapid, because the transition between both units comprises few meters. More importantly, the contact between the Villar del Arzobispo and Aldea de Cortés Fms, previously considered as unconformable, is here interpreted as gradual.

The presence of *Alveosepta* in the Villar del Arzobispo Fm suggests that at least part of this unit is Kimmeridgian, unlike the previously assigned Late Tithonian-Middle Berriasian age. Consequently, the underlying Higueruelas Fm, previously considered Tithonian, should not be younger than Kimmeridgian. Accordingly, sedimentation of the Aldea de Cortés Fm, previously considered Valanginian-Hauterivian, probably started during the Tithonian and it may be considered part of the regressive trend of the Late Jurassic-Early Cretaceous cycle. This is consistent with the dinosaur faunas, typically Jurassic, described in the Villar del Arzobispo and Aldea de Cortés Fms

Keywords: Mixed carbonate-siliciclastic platform, coastal wetland, Foraminifera, Spain, Kimmeridgian, Tithonian

Resumen

El estudio de los depósitos del Jurásico Superior-Cretácico Inferior (formaciones Higueruelas, Villar del Arzobispo y Aldea de Cortés) de la Cuenca Suribérica (NO provincia de Valencia, E España) ha revelado nuevos datos estratigráficos y sedimentológicos, que tienen implicaciones importantes sobre el marco estratigráfico, el ambiente sedimentario y la edad de estas unidades. Además, estos nuevos datos sugieren que se deberían revisar las correlaciones estratigráficas realizadas previamente entre las unidades estudiadas y aquéllas depositadas en otras áreas adyacentes de la Cuenca Ibérica.

La Fm Higueruelas se depositó en la parte media de una plataforma carbonática en la que migraban barras oncolíticas por la acción de las tormentas y en la que la producción de oncolitos disminuía progresivamente hacia la parte alta de la unidad. La Fm Villar del Arzobispo suprayacente ha sido interpretada tradicionalmente como una plataforma interna-lagoon que evolucionó a una llanura mareal. En este

trabajo se reinterpreta como una plataforma carbonática interna afectada por las tormentas y en la que se desarrollaban bajíos oolíticos que protegían un lagoon. Esta plataforma también estaba afectada por la llegada de material siliciclástico del continente. La Fm Aldea de Cortés ha sido interpretada previamente como formada en un lagoon bordeado por llanuras mareales y por llanuras deltaicas fluviales. En este trabajo se reinterpreta como depositada en un humedal costero en el que interaccionaban depósitos lutíticos, cuerpos de agua someros de salinidades dulces a marinas, dunas eólicas y descargas continentales de material siliciclástico.

El contacto entre las Formaciones Higueruelas y Villar del Arzobispo, definido clásicamente como gradual, es interpretado en este estudio como gradual y rápido, ya que la transición entre ambas unidades ocupa muy pocos metros. De forma más importante, el contacto entre las Formaciones Villar del Arzobispo y Aldea de Cortés, considerado previamente como el resultado de una discontinuidad, es interpretado en este trabajo como un contacto gradual.

La presencia de *Alveosepta* en la Fm Villar del Arzobispo sugiere que al menos parte de la unidad presenta una edad Kimmeridgiense, en lugar de la edad previamente asignada de Titoniense superior-Berriasiense medio. Consecuentemente, la edad de la unidad infraya-cente, la Fm Higueruelas, asignada previamente al Titoniense, no sería más moderna que Kimmeridgiense. Por consiguiente, la sedi-mentación de la Fm Aldea de Cortés, atribuida previamente al Valanginiense-Hauteriviense, habría comenzado probablemente durante el Titoniense y debería ser considerada parte de la tendencia regresiva del ciclo Jurásico Superior-Cretácico Inferior. Todo ello está en consonancia con las típicas faunas de dinosaurios encontradas en las formaciones Villar del Arzobispo y Aldea de Cortés, que presentan afinidades jurásicas.

Palabras clave: Plataforma mixta carbonato-siliciclástica, humedal costero, Foraminífera, España, Kimmeridgiense, Titoniense

1. Introduction

The beginning of the Late Jurassic-Early Cretaceous *rifting* cycle affected the carbonate platforms that were previously developing throughout eastern Iberia, producing their break-down and, as a consequence, the arrival to the marine realm of siliciclastic discharges coming from the elevated conti-nental areas (e.g. Aurell *et al.*, 1994; Salas *et al.*, 2001; Mas *et al.*, 2004). As a result, the configuration and depositional patterns of the carbonate platforms changed rapidly, evolv-ing upwards into coastal and continental areas (e.g. Canerot, 1974; Mas *et al.*, 1984, 2004; Díaz and Yébenes *et al.*, 1987; Salas, 1987; Martin-Closas and Serra-Kiel, 1991; Bádenas *et al.*, 2004). In the South Iberian Basin, where this study has been performed (Fig. 1), the oncolitic limestone of the Higueruelas Fm, the limestone, sandstone and claystone of the Villar del Arzobispo Fm and the claystone and sandstone of the Aldea de Cortés Fm, represent the earliest depositional stages of the beginning of the Late Jurassic-Early Cretaceous *rifting* cycle, recording a wide spectrum of mixed siliciclastic and carbonate facies deposited from marine to coastal envi-ronments.

This work revisits these units at the Benagéber area in Los Serranos region (NW Valencia province), where the Al-dea de Cortés Fm was formally defined (Mas, 1981; Vilas *et al.*, 1982), and where detail studies have not been carried out since more than thirty years (Assens *et al.*, 1973; Gómez, 1979; Mas, 1981; Mas and Alonso, 1981; Mas *et al.*, 1984), with the main aim of better understanding the development of the first infilling stages of the South Iberian Basin. The new stratigraphical, sedimentological and paleontological data and interpretations presented here involve important chro-nostratigraphical, paleoenvironmental and paleogeographi-cal implications for the South Iberian Basin during the Late Jurassic-Early Cretaceous. Specifically, new data allow: 1) to precisely characterize the limits between the Higueruelas and Villar del Arzobispo Fms, and to question the contact between the Villar del Arzobispo and Aldea de Cortés Fms,

previously interpreted as an unconformity (e.g. Mas, 1981; Mas and Alonso, 1981; Mas *et al.*, 1982, 2004; Vilas *et al.*, 1982); 2) to make new paleoenvironmental interpretations for the Villar del Arzobispo and Aldea de Cortés Fms, and to qualify those of the Higueruelas Fm; and 3) to modify and improve the accuracy of the ages of these units based on the study of the larger foraminifera present in the Villar del Arzo-bispo Fm. In addition, these new findings will be relevant for a more dating accurate of the historical sites with dinosaurs from Benagéber (see Royo y Gómez, 1926a; 1926b; 1927; Pérez-García *et al.*, 2009) that, taking as reference the loca-tions mentioned in these works, they are included into the Aldea de Cortés Fm in our paper (specifically under the wa-ters of the Turia river in the actual "Embalse de Benagéber").

2. Geological setting

The study area is located in the South Iberian Basin (E Spain, Fig. 1), which is one of the basins of the Mesozoic Iberian Rift System (also referred to as the Iberian Basin) formed during the opening of the North Atlantic Ocean and the Bay of Biscay and was inverted during the Cenozoic Al-pine Orogeny (Salas *et al.*, 2001; Mas *et al.*, 2004). The infill of the South Iberian Basin, which may comprise more than 2000 m of sediments, started in the Tithonian and continued until the Middle Albian (Mas, 1981; Mas and Alonso, 1981; Mas *et al.*, 2004). The South Iberian Basin was surrounded by the Iberian and Valencian Massifs, which were located westwards and northwards of the basin, respectively (Mas *et al.*, 2004). Specifically, the studied deposits crop out in the NW area of the basin, near Benagéber town (NW of Valencia province; Fig. 1) and correspond to the Upper Jurassic-Lower Cretaceous Higueruelas, Villar del Arzobispo and Aldea de Cortés Fms (Fig. 2A).

The lowermost unit, the Higueruelas Fm, has a wide ex-tension throughout the Mesozoic Iberian Rift System and is an oncolitic carbonate unit (67 m thick in the study area), interpreted as shallow subtidal bars deposited in a mid- to
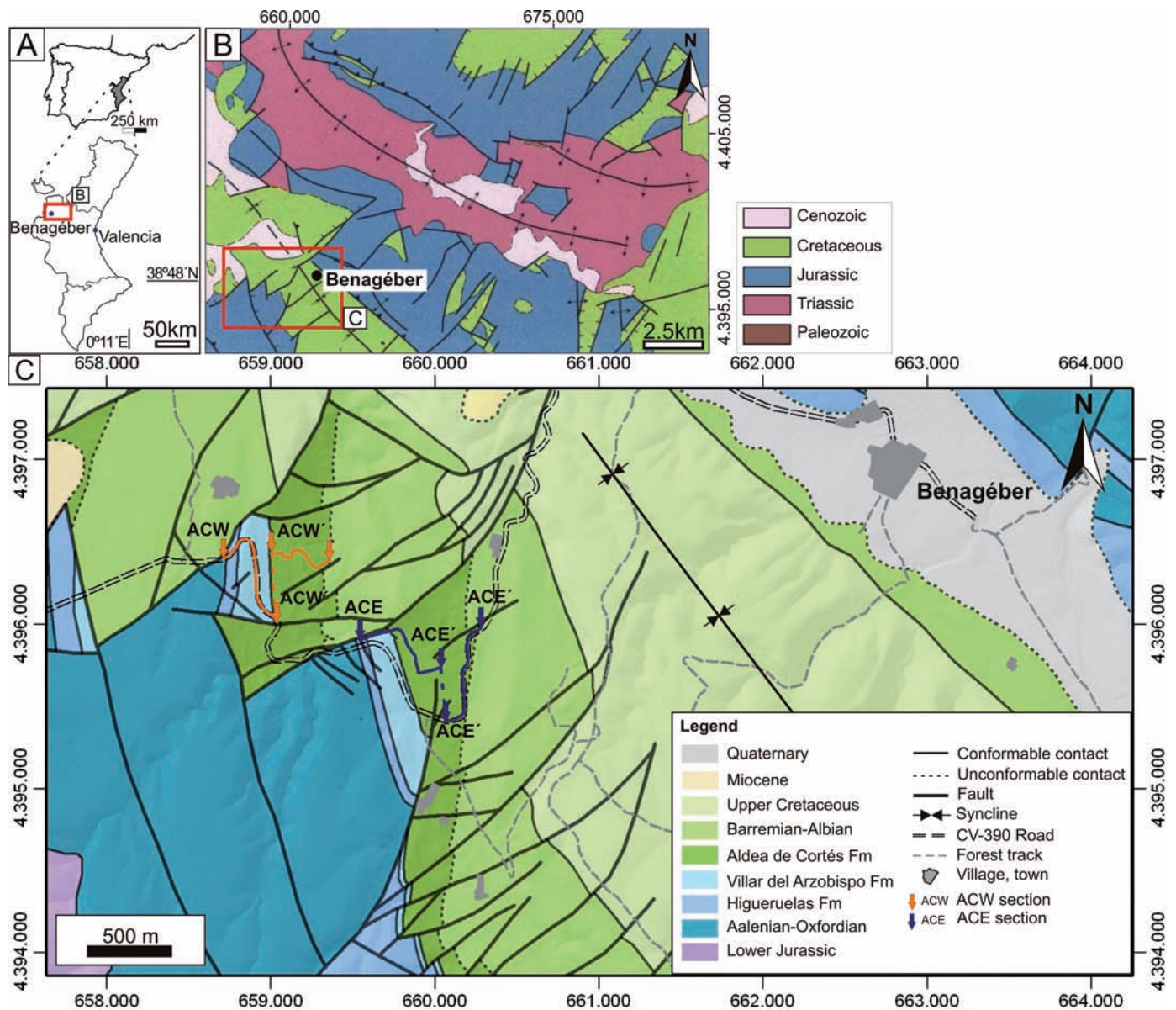
Fig. 1.- Location (A) and geological maps of the study area (B-C). B) Geological map of the NW of Valencia province (modified from Assens *et al.*, 1973). C) Detailed geological map of the area of Benagéber indicating the location of the studied stratigraphic sections (ACW and ACE).

inner-carbonate ramp (e.g. Aurell *et al.*, 1994; Mas *et al.*, 2004). The Villar del Arzobispo Fm lies conformably over the Higueruelas Fm and, in the study area, it comprises up to 110 m of mixed carbonate-clastic deposits previously interpreted as deposited in an inner ramp-lagoon environment, which evolved upwards into a tidal flat system (Mas and Alonso, 1981; Mas *et al.*, 1984; 2004). The uppermost unit, the Aldea de Cortés Fm (Fig. 2A), has traditionally been considered as unconformable over the Villar del Arzobispo Fm (Mas, 1981; Mas and Alonso, 1981; Vilas *et al.,* 1982; Mas *et al.*, 1984; 2004) and, in the study area, it comprises more than 200 m of siliciclastic sediments with minor carbonates, previously interpreted as deposited in lagoons, tidal flats and fluvial deltaic plains (Mas, 1981; Mas and Alonso, 1981; Mas *et al.*, 1982; 2004; Vilas *et al.*, 1982).

The age of the studied stratigraphic units is controversial due mainly to the scarcity or even lack of ammonoids and other pelagic fossils commonly used for establishing the chronostratigraphic ages in Global Time Scales (see Gradstein *et al.*, 2012 and references therein). However, previous regional works about the studied deposits have used other neritic groups (e.g. larger foraminifera) to assess the age of the units. Thus, the Higueruelas Fm was assigned to the "Middle" Kimmeridgian (Fig. 2B; Gómez, 1979; Gómez and Goy, 1979) or "Middle"-Upper Kimmeridgian (Fig. 2B; Viallard, 1973; Ramírez del Pozo in Assens *et al.*, 1973) based on the presence of the larger foraminifera association of *Alveosepta jaccardi* (Schrodt), *Everticyclammina virguliana* (Koechlin)*, Pseudocyclammina cf. lituus* (Yokohama), *Kurnubia palastiniensis* Henson and *"Labyrinthina" mirabilis* (Fourcade and
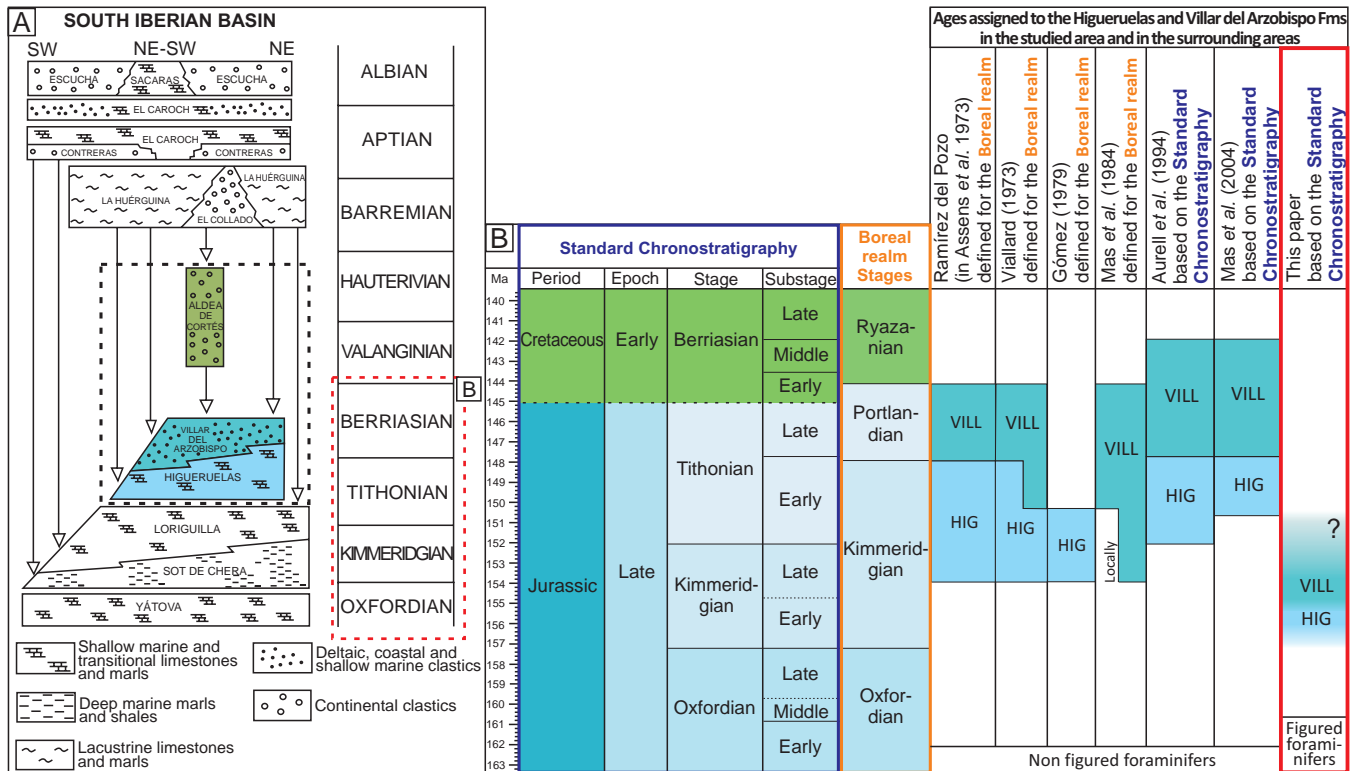
Fig. 2.- A) Chrono-lithostratigraphic diagram for the South Iberian Basin (modified from Salas *et al.*, 2001). The studied geological units are colored and they comprise the Tithonian-Berriasian record (the Higueruelas and Villar del Arzobispo Fms) and the Valanginian-Hauterivian record (the Aldea de Cortés Fm). B) Oxfordian to Berriasian chronostratigraphy modified from Gradstein *et al.* (2012). The table shows the Standard Chronostratigraphy and its correlation with the Boreal realm stages defined in Great Britain. The table also includes the different ages previously assigned to the Higueruelas and Villar del Arzobispo Fms in the study area and in the surrounding zones, and the age proposed in this paper.

Neumann). The overlying Villar del Arzobispo Fm contains an association of larger foraminifera dominated by *Anchispirocyclina lusitanica* (Egger), allowing the assignment of this unit to the Portlandian (Fig. 2B; Ramírez del Pozo in Assens *et al.*, 1973) or to the Upper Kimmeridgian-Portlandian (Fig. 2B; Viallard, 1973; Mas and Alonso, 1981; Mas *et al.*, 1984). However, Viallard (1973), Mas and Alonso (1981) and Mas *et al.* (1984) mentioned the local occurrence of *Alveosepta jaccardi* at the basal strata of some sections of the Villar del Arzobispo Fm, and therefore a possible Kimmeridgian age was suggested for the basal strata of this unit (Fig. 2B).

In the following years, and after the acceptance of the Tithonian as a stage by the International Commission on Stratigraphy in 1990, several authors tried to adapt the "old" ages to the new global scales in their regional works, leading to problematic interpretations. In this sense, Aurell *et al.* (1994; 2002) and Mas *et al.* (2004), based on the same fossils previously mentioned, attributed the Higueruelas Fm to the Tithonian and the Villar del Arzobispo Fm to the Late Tithonian-Middle Berriasian, in an attempt to adapt the Boreal ages to Mediterranean stages, firstly and to the Global Time Scale, later (Fig. 2B).

The Aldea de Cortés Fm has been attributed to the Valanginian-Hauterivian based only on the ages of its underlying and overlying geological units (Fig. 2A) but no paleontological data support this age (Mas, 1981; Mas y Alonso, 1981; Mas *et al.*, 1982; 1984; 2004; Vilas *et al.*, 1982).

3. Methodology

This research is based on the geological mapping and the stratigraphic, petrographic and paleontological analysis of the Higueruelas, Villar del Arzobispo and Aldea de Cortés Fms. Geological mapping was performed using field observations, aerial photographs and satellite images (Fig. 1). The acquired data were integrated and georeferenced with ArcGIS software.

Two stratigraphic sections (named ACW and ACE; Fig. 3) were logged in the areas with best outcrop conditions (Fig. 1). The three studied units outcrop completely in the ACW section, whereas in the ACE section, the lowermost part of the Higueruelas Fm does not outcrop due to the presence of a fault at the base of this section.

A total of 140 rock samples were collected systematically along the stratigraphic sections, as well as in areas with special sedimentological and paleontological interest. A polished and uncovered thin section (30 µm thick) was prepared for each rock sample, in order to carry out a petrological study. Petrographic and sedimentological descriptions were based on the classification of carbonate rocks of Dunham (1962)

FACIES		COMPONENTS	STRUCTURES	ENVIRONMENTAL INTERPRETATION
F1. Oncolitic packstone		Oncoids (mainly discontinuous laminae), fecal pellets, small agglutinated forams and miliolids, fragments of serpulids, echinoderms, ostreids and other bivalves, gastropods, brachiopods, corals and sponges.	Large-scale cross-bedding	Transport by unidirectional tractive currents below the fair-weather wave base and above the storm wave base, under normal marine salinity waters. Alternance of high and low agitation periods.
F2.	**F2A. Peloidal packstone**	Fecal pellets, scarce small agglutinated forams and miliolids. Scarce fragments of bivalves, brachiopods, echinoderms and ostracods.	Not observed	Production of fecal pellets in low-agitation waters.
	F2B. Rippled peloidal packstone	Fecal pellets, minor micritic intraclasts, scarce small agglutinated forams and miliolids, fragments of bivalves, brachiopods, echinoderms, serpulids, ooids and quartz grains.	Wave and/or current ripples	Fecal pellets, minor intraclasts and fossil remains reworked by wave and tractive currents.
F3. Oncolitic packstone-grainstone and grainstone		Oncoids (mainly continuous laminae), fecal pellets, micritic intraclasts, small agglutinated forams, small miliolids, fragments of gastropods, bivalves (ostreids and other bivalves), brachiopods, corals, echinoderms, chaetetids, stromatoporoids, sponges and serpulids.	Not observed	Transport by continuously agitated currents above the fair-weather wave base and under normal marine salinity waters.
F4. Peloidal and bioclastic packstone-grainstone		Fecal pellets, fragments of echinoderms, brachiopods, bivalves (ostreids and other bivalves), corals, gastropods, sponges, small agglutinated forams, small miliolids, solenoporacean red algae and intraclasts. Bioclasts and intraclasts show incipient thin continuous oncolitic laminae.	Large-scale cross-bedding	Transport by unidirectional tractive currents above the fair-weather wave base and under normal marine salinity waters.
F5. Very fine to fine-grained sandstone	**F5A**	Quartz, feldspar, micritic intraclasts, minor muscovite, biotite, chlorite, scarce tourmaline and plant remains. Locally contains up to 15% of bioclasts (fragments of ostreids and other bivalves, echinoderms, serpulids, brachiopods, gastropods, small agglutinated forams, small miliolids, sponges) and ooids.	Parallel lamination (plane bed)	Transport by upper flow regime tractive currents.
	F5B		Large-scale cross-bedding	Transport by lower flow regime unidirectional tractive currents.
F6. Oolitic packstone-grainstone		Ooids, quartz grains, small and large agglutinated forams, small miliolids, fragments of gastropods, echinoderms, bivalves dasycladales, intraclasts, fecal pellets and scarce oncoids.	Large-scale cross-bedding	Transport by unidirectional tractive currents above the fair-weather wave base and under marine normal waters. Siliciclastic input.
F7. Mudstone		Scarce small and large agglutinated forams, small miliolids, fragments of bivalves, gastropods, brachiopods and echinoderms.	Not observed	Micrite precipitation and accumulation under calm conditions.
F8. Bioclastic and peloidal packstone and packstone-grainstone	**F8A**	Small and large agglutinated forams, small miliolids, trocholinids, fragments of echinoderms, gastropods, serpulids, dasycladales, bivalves, ostracods, solenoporacean red algae, ostreids, quartz grains, fecal pellets, scarce ooids, oncoids and vertebrate remains.	*Thalassinoides*-like and *Rhyzocoralium* traces	Transport by episodic currents. Siliciclastic input.
	F8B	Quartz grains, fragments of charophytes, ostracods, gastropods, ostreids and other bivalves, scarce echinoderms, small agglutinated forams and miliolids, vertebrate remains, fecal pellets, intraclasts and scarce ooids. Locally, fragments of bivalves are rounded to subrounded.	*Thalassinoides*-like traces. Locally, bivalves oriented parallel to bedding.	Transport by episodic currents and locally reworked by tractive currents. Influence of both fresh and seawaters. Siliciclastic input.
F9. Marl		Siliciclastic mudstone and micrite	Not observed	Suspended-load decantation processes and $CaCO_3$ precipitation.
F10. Siliciclastic mudstone		Siliciclastic mudstone	Grey and red colors. Carbonate nodules. Green mottling.	Suspended-load decantation and edaphic alteration.
F11. Very fine- to medium-grained sandstone	**F11A**	Quartz, feldspar, micritic intraclasts, minor muscovite, biotite, chlorite, scarce tourmaline and plant remains.	Current and wave ripples	Locally *Thalassinoides*-like trace	Transport by tractive currents.
	F11B		Large-scale cross-bedding		Transport by lower flow regime unidirectional tractive currents.
	F11C		Parallel lamination (plane bed)		Transport by upper flow regime tractive currents.
F12. Cross-bedded sandstone	**F12A. Fine- to medium-grained**	Quartz, feldspar, micritic intraclasts, minor muscovite, biotite and tourmaline.	Sigmoidal-like stratification	Sediment entering stagnant water bodies transported by tractive currents (i.e. sediment lobes).
	F12B. Coarse- to very coarse-grained	Quartz, feldspar, micritic intraclasts, minor muscovite, biotite and tourmaline. Scatter carbonate pebbles.		
F13. Cross-bedded conglomerate		Carbonate clasts (0.2-1.6 cm in diameter) within a coarse to very coarse sandy matrix, large fossil plant trunks, ooids.	Large-scale cross-bedding	Transport by unidirectional tractive currents.
F14. Massive clast-supported conglomerate		Carbonate and quartzite clasts (0.2-5 cm in diameter) within a fine to medium-grained sandy matrix. Fragments of bivalves, ooids, vertebrate remains and large fossil plant trunks.	Not observed	Transport by ephemeral currents
F15. Fine–to medium-grained well to very well-sorted, cross-bedded sandstone	**F15A**	Quartz, feldspar, muscovite, biotite, chlorite. Muddy soft pebbles and plant remains.	Wedge-shaped sets Large-scale cross-bedding High angle foresets Low angle foresets and large lateral continuous bottomsets. Bottomsets and occasionally the lower part of the low angle foresets draped by mica flakes and plant remains Reactivation surfaces	Deposition of aeolian dunes. Local decantation of suspended load in wet interdunes.
	F15B		Wave and current ripples at the bottomsets	Reworking by waves and tractive currents in wet interdunes.

Table1.- Facies distinguished in the stratigraphic sections ACE and ACW.

FACIES ASSOCIATION		FACIES	ENVIRONMENTAL INTERPRETATION
Higueruelas Fm			
A: Oncolitic and peloidal facies association	**A1**	Oncolitic packstone facies (F1), changing upwards gradually and rapidly to the peloidal packstone facies (F2A).	Oncoid shoals migrating by the action of storms in the mid-carbonate platform under marine normal waters. Oncoid shoals protected calm areas where invertebrate organisms produced fecal pellets.
	A2	Oncolitic packstone-grainstone and grainstone facies (F3) changing gradually and rapidly upwards to the rippled peloidal packstone (F2B).	Oncoid shoals in the inner-carbonate platform under marine normal waters. Oncoid shoals protected areas where invertebrate organisms produced fecal pellets, which were reworked by tractive currents.
B: Peloidal and bioclastic facies association		Peloidal and bioclastic packstone-grainstone facies (F4) changing gradually and rapidly to the rippled peloidal packstone facies (F2B).	Bioclastic and peloidal shoals in the inner-carbonate platform under marine normal waters. Bioclastic and peloidal shoals protected areas where invertebrate organisms produced fecal pellets, which were reworked by wave and tractive currents.
Villar del Arzobispo Fm			
C: Sandstone facies association		Very fine- to fine-grained sandstone displaying parallel lamination (F5A) at the base and large-scale cross-bedding at the upper part (F5B)	Siliciclastic discharges coming from the emerged areas and deposited in the inner-carbonate platform, where they were reworked by storms.
D: Oolitic and peloidal facies association	**D1**	Oolitic packstone-grainstone facies (F6) changing gradually and rapidly upwards to the peloidal packstone facies (F2A), the rippled peloidal packstone facies (F2B) or the mudstone facies (F7)	Oolitic shoals developed in the inner-carbonate platform under marine brackish waters. Oolitic shoals protected areas where invertebrate organisms produced abundant fecal pellets and where micrite accumulated under calm conditions.
	D2	Oolitic packstone-grainstone facies (F6) changing gradually upwards to the bioclastic and peloidal packstone and packstone-grainstone facies (F8A).	Oolitic shoals developed in the inner part of a carbonate platform under marine brackish normal waters. Oolite shoals protected agitated areas that received freshwater inputs.
E: Marl-limestone-sandstone facies association		Marl (F9), interbedded with bioclastic and peloidal packstone and packstone-grainstone facies (F8A) and occasionally with fine- to medium- grained sandstone (F11 and F12A)	Shallow, protected and brackish lagoon affected by the arrival of neighboring marine carbonate deposits transported by storms and also of siliciclastic discharges coming from elevated areas.
Aldea de Cortés Fm			
F: Siliciclastic mudstone-sandstone facies association		Siliciclastic mudstone (F10) interbedded with minor very fine- to fine- grained sandstone (F11 and F12A)	Flood plain that underwent periodical subaerial exposure and development of vegetation, which received siliciclastic discharges coming from elevated areas.
G: Coarse- to very coarse-grained sandstone and conglomerate facies association		Cross-bedded coarse- to very coarse- grained sandstone (F12B) and conglomerate (F13, F14), interbedded with siliciclastic mudstone (F10)	Siliciclastic discharges coming from elevated continental areas, transported by ephemeral currents and deposited in a flood plain.
H: Limestone facies association		Peloidal packstone and packstone-grainstone (F8B) interbedded with siliciclastic mudstone (F10)	Shallow and ephemeral water bodies, influenced by both fresh and marine waters, developed in a coastal plain and formed during storms or flooding episodes.
I: Large-scale cross-bedded sandstone facies association		Fine- to medium-grained, well- to very well-sorted, cross-bedded sandstone (F15) interbedded with siliciclastic mudstone (F10)	Aeolian dunes and interdunes.

Table 2.- Facies associations distinguished in the stratigraphic sections ACE and ACW.

and the classification of siliciclastic rocks of Zuffa (1980). For the oncolitic deposits of the Higueruelas Fm, the description of the microfabrics observed in the oncolitic laminae is based on the terminology used by Dahanayake (1977) for the Kimmeridgian oncoids of the French Jura Mountains.

The paleontological study is based on ten samples (Ac1027, Ac1029, Ac1031, Ac1033, Ac1035, ACE011-014, ACE016) from several levels of the Villar del Arzobispo Formation (Fig. 3). No paleontological content of biostratigraphic relevance has been found in the underlying Higueruelas Fm and the overlying Aldea de Cortés Fm (see the facies description). From these ten samples, 17 thin sections were prepared, and the foraminiferal content was analyzed, with special attention to the larger foraminifera. About twenty random sections of

Alveosepta personata (Tobler) have been obtained associated to few and bad preserved sections of *Kurnubia* sp., "*Labyrinthina*" *mirabilis* (Fourcade and Neumann), small and flat trocholinids, *Nautiloculina oolithica* Mohler, small miliolids and small agglutinated benthic foraminifera. All the material collected for this research is held at the Stratigraphy Department of the Complutense University of Madrid (Spain).

Paleocurrent data were represented in rose diagrams with PAST software (Hammer *et al.*, 2001), which show paleocurrent senses grouped in classes of 15º. The relative abundance of paleocurrent measurements in each class is represented by the length of each sector. The total number of paleocurrent measurements is indicated on the upper right part of each roses diagram with letter "n" (Figs. 5B, 8F). For obtaining
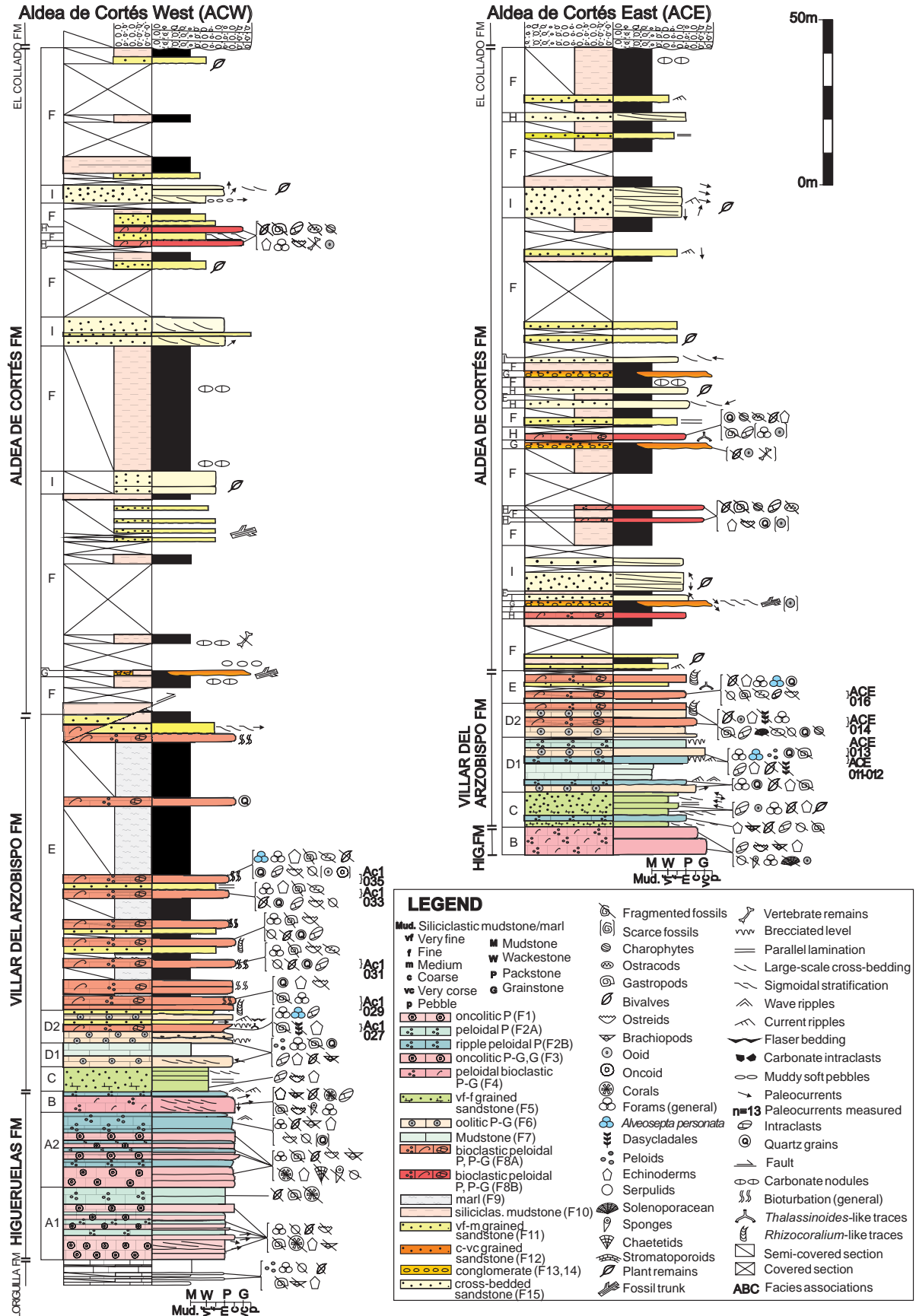
Fig. 3.- Stratigraphic sections measured in the study area (Aldea de Cortés West, ACW, and Aldea de Cortés East, ACE) comprising the Higueruelas, Villar del Arzobispo and Aldea de Cortés Fms (see Fig. 1 for location). Left column indicates the different facies associations (see text and Table 2 for explanation). Samples selected for the paleontological study are indicated in the right part of each section.

final paleocurrent values, the tectonic dip was discounted using the sterographic projection.

4. Facies analysis

Fifteen carbonate and siliciclastic facies have been distinguished (Table 1, Fig. 3) and have been grouped into nine facies associations (two facies associations in the Higueruelas Fm, three in the Villar del Arzobispo Fm and four in the Aldea de Cortés Fm, Table 2), representing different depositional environments, which are described and interpreted below.

4.1. Higueruelas Fm facies associations (Fig. 4)

The Higueruelas Fm outcrops in both stratigraphic sections; in the ACW section, this unit outcrops completely, whereas only its uppermost part is observed in the ACE section (Fig. 3).

A: Oncolitic and peloidal facies association

This facies association only occurs in the lower and middle parts of the Higueruelas Fm in the stratigraphic section ACW (Fig. 3) and has been subdivided into two facies subassociations:

Facies subassociation A1. The facies subassociation A1 is observed in the lower part of Higueruelas Fm (Fig. 3). It is composed of fining-upwards sequences of 2.20-5.30 m in thickness with flat or slightly irregular bases and tops (Fig. 4A). Sequences start with oncolitic packstone facies (F1), changing upwards, gradually but rapidly, within few centimeters, to peloidal packstone facies (F2A).

The oncolitic packstone facies (F1) is arranged in decimeter to meter thick massive beds (up to 2.40 m) with occasional and poorly-preserved large-scale cross-bedding (paleocurrents towards the E-NE, Fig. 4A). Components of this facies are: oncoids, fecal pellets and bioclasts (Fig. 4D-F). Fecal pellets show homogeneous sizes (50-200 µm), rounded to elliptical sections and display, occasionally, an internal sieve-like structure. Bioclasts are small agglutinated forams and miliolids, fragments of serpulids, echinoderms, ostreids and other bivalves, gastropods, brachiopods, corals and sponges. Oncoids show rounded or slightly elliptical sections and are 0.5-2.5 cm in size, although in each bed, oncoids typically show homogeneous sizes. Oncoid nuclei are usually one of the bioclasts mentioned above or intraclasts, and occasionally they show compound nuclei. The cortex of the oncoids is mainly formed by discontinuous concentric laminae (Fig. 4E-F) and, less commonly, by continuous laminae. Laminae are composed of different microfabrics: 1) Dense micritic microfabric. 2) Grumose microfabric composed of 15-100 µm size micritic aggregates separated by sparite cement. 3) Organism-bearing microfabric formed by micrite or micritic aggregates and encrusting organisms (serpulids, nubecularid forams, *Troglotella incrustans* Wernli and Fookes, *Lithocodium aggregatum* El-

liot and *Bacinella irregularis* Radoicic) and/or fragmented bioclasts. These microfabrics may occur in different laminae of the same oncoid.

The peloidal packstone facies (F2A; see Fig. 4G) is composed of fecal pellets (20-100µm), and scarce small agglutinated forams and miliolids and slightly fragmented fossil remains (<10%): bivalves, brachiopods and echinoderms. No tractive structures have been observed within this facies.

Interpretation of facies subassociation A1

Oncolitic deposits (F1) of the *facies subassociation A1* are interpreted as deposited in subtidal oncoid shoals which migrated in a carbonate platform and under normal marine salinity waters, due to their fossil content. The fact that oncoid laminae are mostly discontinuous indicates that oncoids remained static under calm periods, allowing microbial mats and/or encrusting organisms to colonize the surface of the oncoid that was not in contact with the sediment. Episodes of agitation were also required to turn the oncoids over, allowing the colonization of the rest of their surface (e.g. Dahanayake, 1977). This alternation of calmed and agitated episodes suggests that the oncolitic deposits were affected by episodic currents such as storm currents. Similar oncolitic deposits have been previously described in the Higueruelas Fm in other areas of the Iberian Basin and have been interpreted as oncoid shoals subjected to the action of episodic storms in the middle ramp of a storm-dominated carbonate platform (Aurell *et al.*, 1994; 1999; Ipas *et al.*, 2004). Comparable oncolitic deposits have been also described in the Late Kimmeridgian Torrecilla Fm in other sectors of the Iberian Basin (Zaragoza and Teruel provinces), where they have been interpreted as deposited in the middle ramp of a carbonate platform affected by storms (Bádenas *et al.,* 1993; Bádenas and Aurell, 2004; 2010), which produced undertow currents out to the sea, located eastwards (Bádenas, 1999; Aurell *et al.*, 1995; Bádenas and Aurell, 2001b).

The peloidal packstone facies (F2A) is interpreted as deposited under calm conditions, in "shadow areas", according to Gómez (1979) and Aurell (1990), developed between the oncoid shoals, where invertebrate organisms, such as crustaceans, gastropods, bivalves, and brachiopods, among others, produced abundant fecal pellets (e.g. Tucker and Wright, 1990; Flügel, 1982; 2010).

The dominant discontinuous nature of oncoid laminae, which were transported episodically by storm currents, and the lack of tractive structures in the peloidal facies (F2A) suggest that the *facies subassociation A1* was deposited in the mid-carbonate platform below the fair-weather wave base and above the storm wave base.

Facies subassociation A2. The facies subassociation A2 is observed in the middle part of the Higueruelas Fm (Fig. 3). It is composed of fining-upwards sequences, 1.50-7.5 m thick, with flat or slightly irregular bases and tops (Fig. 4B), which start with oncolitic packstone-grainstone and grainstone facies (F3) and change upwards gradually and rapidly, within few centimeters, to rippled peloidal packstone (F2B).
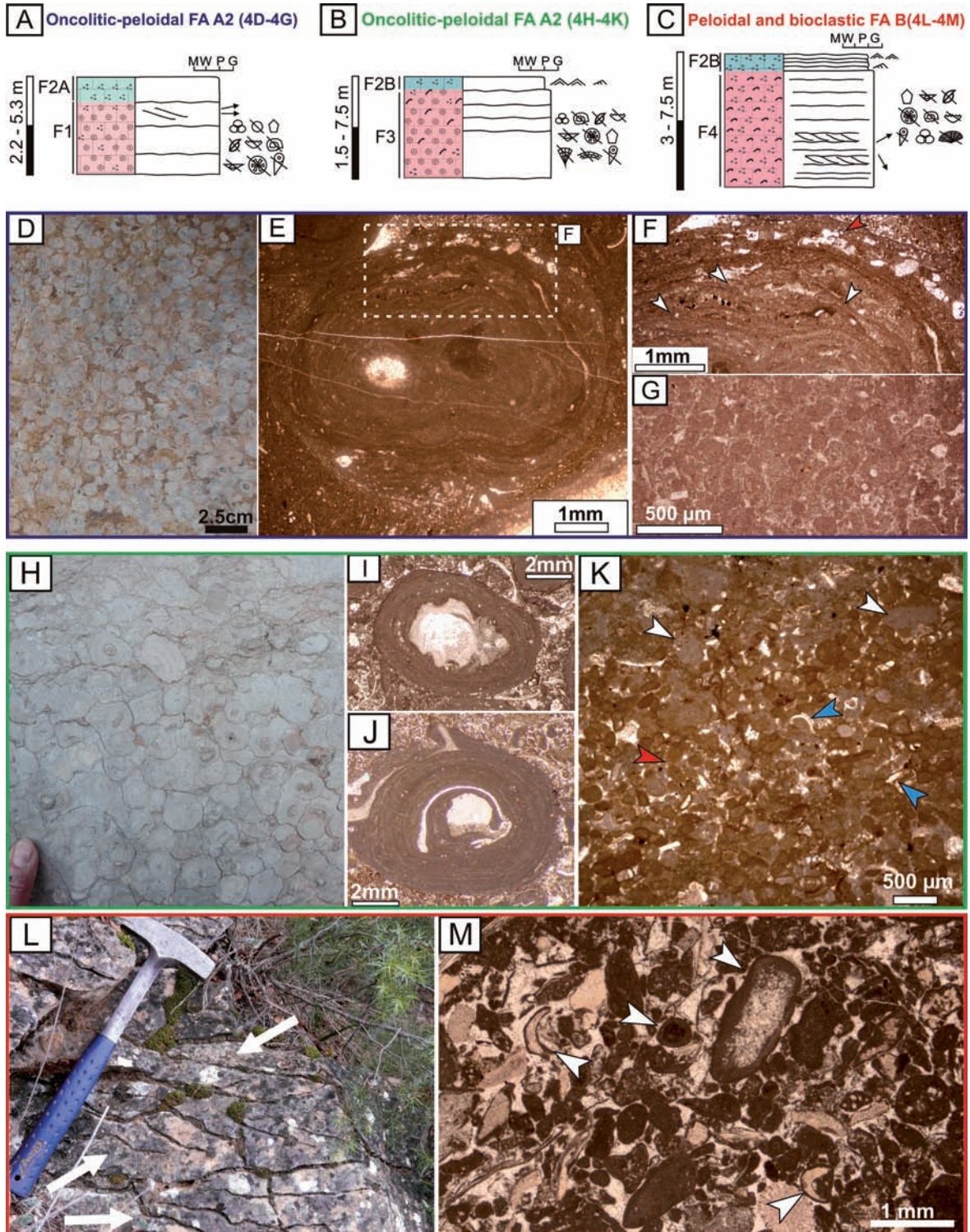
Fig. 4.- Facies associations of the Higueruelas Fm. A, D-G) Oncolitic-peloidal facies subassociation A1: A) Characteristic sequence of the facies subassociation A1. See Fig. 3 for legend. D) Field photograph of oncoid packstone facies (F1). E) Transmitted light (TL) micrograph of an oncoid of the oncolitic packstone facies (F1) mainly formed by discontinuous laminae. F) Detail of the discontinuous laminae with micritic microfabric or organism bearing microfabric (*Lithocodium* red arrow). Note that laminae get thiner at their endings (white arrows). G) Detail of the fecal pellets of the peloidal packstone facies (F2A) showing submillimetric and homogeneous sizes, and rounded to elliptical shapes. B, H-K) Oncolitic-peloidal facies subassociation A2: B) Characteristic sequence of the facies subassociation A2. See Fig. 3 for legend. H) Field photograph of the oncolitic packstone-grainstone and grainstone deposits (F3).- I-J) TL micrographs of the oncoids of facies F3. Note that most laminae are continuous around the oncoids. K) TL micrograph of the rippled peloidal packstone facies (F2B) with homogeneous and submillimetric fecal pellets (red arrow), irregular and less homogeneous micritic intraclasts (white arrows) and fossil remains (blue arrows). C, L-M) Peloidal and bioclastic facies association B: C) Characteristic sequence of the facies association B. See Fig. 3 for legend. L) Field photograph of the peloidal and bioclastic packstone-grainstone facies (F4), displaying large-scale cross-bedding (arrows). M) TL micrograph of the peloidal and bioclastic packstone-grainstone facies (F4). Intraclasts and bioclasts show thin incipient oncolitic laminae (arrows).
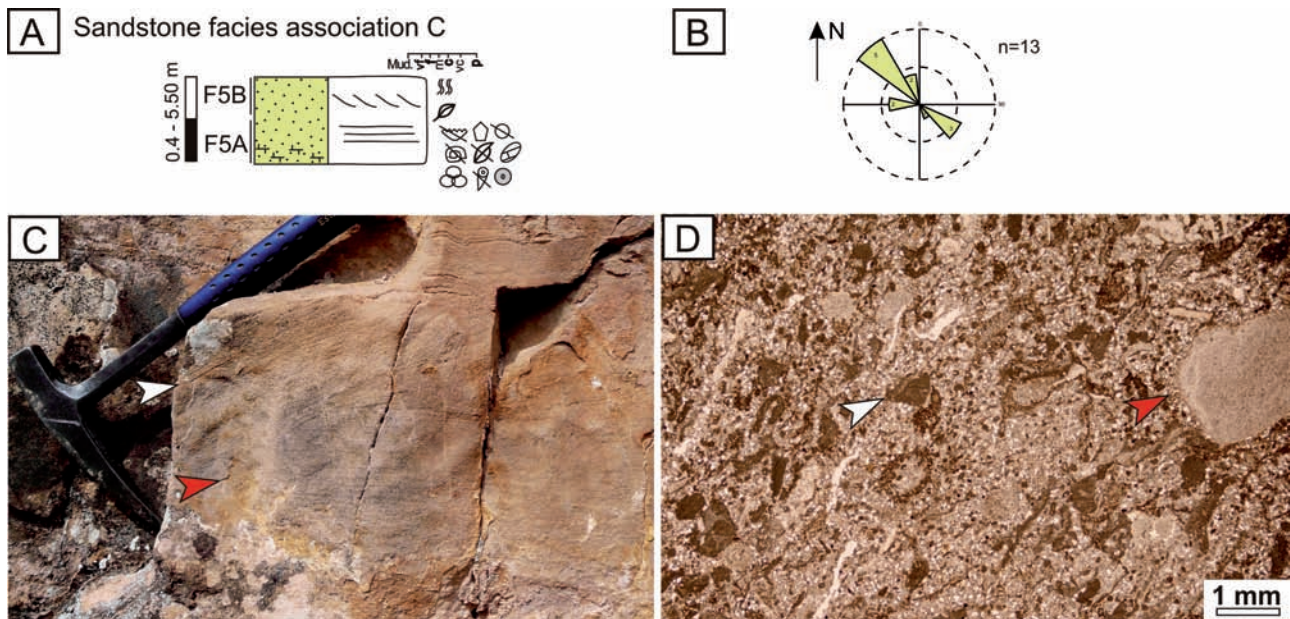
Fig. 5.- Sandstone facies association C of the Villar del Arzobispo Fm. A) Characteristic sequence of the facies association C. See Fig. 3 for legend. B) Paleocurrent measurements show a predominant transport towards the NW and a secondary transport towards the SE. C) Field photograph of the characteristic structures observed in this facies association: parallel lamination at the base (red arrow), and large-scale cross-bedding towards the top of the sequences (white arrow). D) TL micrograph of hybrid arenites with irregular intraclasts (white arrow) and echinoderms (red arrow).

The oncolitic packstone-grainstone and grainstone facies (F3; Fig. 4B, H, J) is arranged in meter thick beds and it includes: oncoids, homogeneous and submillimetric fecal pellets (50-200 µm), micritic intraclasts (50-200 µm), and the same bioclasts mentioned in *facies subassociation A1* but including irregular and angular fragments of chaetetids and stromatoporids (up to 7 cm in size). Oncoids show rounded or slightly elliptical sections and are 0.5-2 cm in size, but in each bed oncoids typically show homogeneous sizes. Oncoid nuclei are formed by one of the bioclasts mentioned above or by an intraclast. The oncoid cortices are mainly formed by continuous concentric laminae (Fig. 4I-J) of micritic and grumose microfabrics. Less abundant discontinuous laminae of organism-bearing microfabric are also observed. The rippled peloidal packstone facies (F2B; see Fig. 4K) is mainly composed of fecal pellets (50-100µm), but in contrast to facies F2A, it also contains minor micritic intraclasts (50-200µm), scarce small agglutinated forams and miliolids, scarce highly

fragmented fossil remains (bivalves, brachiopods, echinoderms and serpulids) and scarce quartz grains (<5%) and, in addition, displays current and wave ripples.

Interpretation of facies subassociation A2

The nature of the oncoid cortices of facies F3, mainly formed by continuous concentric laminae, required constant agitated conditions to rotate the oncoid regularly, in order to develop the same microfabric around the entire oncoid surface. This fact, together with the nature of the fossil content and the packstone-grainstone to grainstone texture, indicate that these deposits were developed in oncolitic shoals, which migrated in the inner-carbonate platform under normal marine salinity waters with continuous agitation and thus, above the fair-weather wave base. This interpretation is in accordance with features of the peloidal packstone facies F2B (highly fragmented fossils and wave and current ripples), which suggest that they were reworked by tractive currents. Moreover, this interpretation is also consistent with that proposed for the

Fig. 6.- (next page) Carbonate and mixed carbonate and siliciclastic facies associations D of the Villar del Arzobispo Fm. A-C) Oolitic-peloidal facies subassociation D1: A) Characteristic sequence of the oolitic-peloidal facies subassociation D1. See Fig. 3 for legend. B) Field photograph of the oolitic packstone-grainstone facies (F6) with cross-bedding (white arrows). C) TL micrograph of the ooids with radial and micritic structures. The nuclei are mainly quartz grains, micritic carbonate particles and bioclasts. D-N) Oolitic-peloidal facies subassociation D2: D) Characteristic sequence of the oolitic-peloidal facies subassociation D2. See Fig. 3 for legend. E) Base of the facies subassociation D2 sequence, showing an accumulation of angular and heterometric carbonate intraclasts (white arrow). F) Top of a sequence showing brecciated appearance. The breccia is composed by heterometric carbonate intraclasts within an orange-colored very fine-grained sandstone matrix. G) Microscopic detail of the bioclastic and peloidal facies (F8A), in which foraminifers are the most abundant fossil remains: small miliolids (1), large agglutinated forams (2). H-M) Dasycladales observed in the bioclastic and peloidal facies (F8A): *Salpingoporella granieri* (H-I), *Salpingoporella annulata* (J-K) and *Holosporella* (L-M) (Dr. I. Bucur pers. comm.). N) Thickening and coarsening-upwards siliciclastic sequences (white bracket) that locally overlie the carbonates of facies subassociation D2 (red arrow). O-Q) Marl-limestone-sandstone facies association E: O) Characteristic sequence of the marl-limestone-sandstone facies association E. See Fig. 3 for legend. P) Outcrop detail of the bioclastic and peloidal packstone and packstone-grainstone facies (F8A) showing *Rhizocorallium*-like traces (1) and large fragments of ostreids (2). Q) Sandstone beds with sigmoidal-like stratification, which occur between marl.

Oolitic-peloidal facies subassociation D1
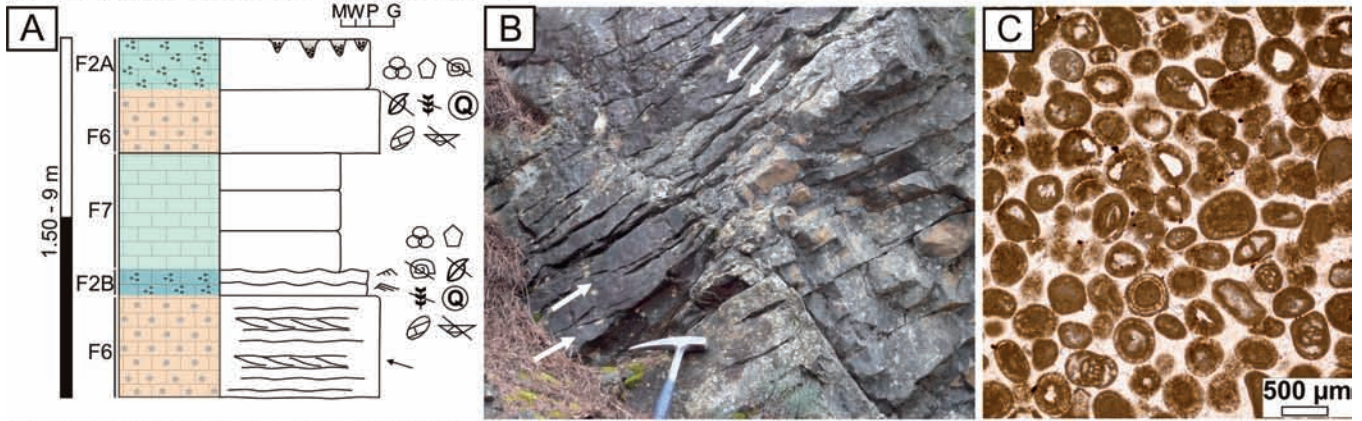
Oolitic-peloidal facies subassociation D2
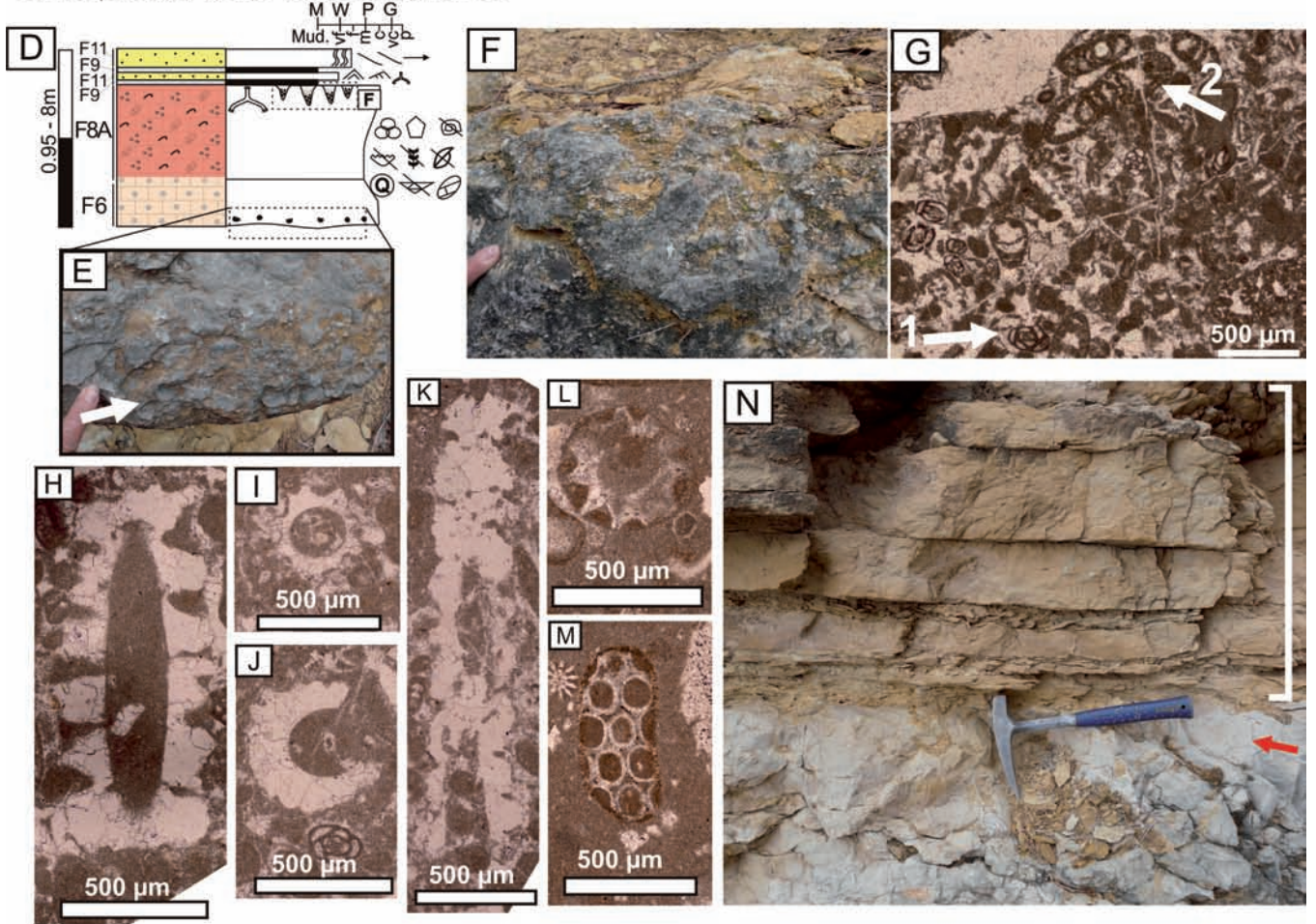
Marl-limestone-sandstone facies association E

oncolitic deposits of the Higueruelas Fm (Aurell, 1990; Aurell *et al.*, 1994) and the Torrecilla Fm (Bádenas and Aurell, 2010) in other sectors of the Iberian Basin, which have been interpreted as oncolitic shoals developed in highly agitated open-marine areas around or above the fair-weather wave base in the inner-ramp of a carbonate platform.

B: Peloidal and bioclastic facies association

This facies association is observed in the upper part of the Higueruelas Fm in both stratigraphic sections (Fig. 3). It is formed by fining-upwards sequences of 3-7.5 m in thickness with flat or slightly irregular bases and tops (Fig. 4C). The sequences start with peloidal and bioclastic packstone-grainstone facies (F4), which change gradually and rapidly to rippled peloidal packstone facies (F2B).

The peloidal and bioclastic packstone-grainstone (F4; see Fig. 4C, L-M) is arranged in meter thick massive beds with occasional large-scale cross-bedding (Fig. 4L) showing paleocurrents pointing towards the NE and SE (Fig. 4C). It is mainly composed of homogeneous and submillimetric fecal pellets (50-250 µm), bioclasts (fragments of echinoderms, brachiopods, bivalves, corals, gastropods, ostreids, sponges, small agglutinated forams and miliolids, and solenoporacean red algae) and sub-rounded to rounded submillimeter-sized (50-700 µm) carbonate intraclasts, which have mudstone, bioclastic wackestone, or peloidal packstone textures. Bioclasts and intraclasts commonly show incipient thin continuous oncolitic laminae of micritic and grumose microfabrics (Fig. 4M).

Rippled peloidal packstone facies (F2B) is formed by fecal pellets (50-100 µm), minor micritic intraclasts (50-500 µm), quartz grains (10-15%), scarce small agglutinated forams and miliolids, scarce highly fragmented fossil remains (bivalves, echinoderms and serpulids) and scarce ooids. Wave and current ripples are observed in this facies.

Interpretation of facies association B

The packstone-grainstone texture, the presence of tractive structures (large-scale cross-bedding), the incipient continuous oncolitic laminae and the fossil content of the peloidal and bioclastic facies (F4) suggest that they were deposited above the fair-weather wave base and under normal marine salinity waters, as the result of the migration of peloidal and bioclastic shoals in the inner-carbonate platform. The decrease of the oncoid cortices thickness in relation to those of the *oncoid and peloidal facies association A*, indicates a progressive upwards decrease of oncoid development. Comparable interpretations are given for similar deposits of the Higueruelas Fm in other areas of the Iberian Basin (Zaragoza province) by Ipas *et al.* (2004). Similar deposits have been also described in the Bovalar Fm (middle Tithonian-early Berriasian) at the Penyagolosa sub-basin (Maestrat Basin), which have been interpreted as highly-agitated shoals developed in the inner ramp of a carbonate platform (Bádenas *et*

al., 2004). On the other hand, features of the rippled peloidal packstone facies (F2B) indicate that these deposits, developed between the shoals, were also reworked by tractive currents, as interpreted for the *oncoid and peloidal facies subassociation A2*.

4.2. Villar del Arzobispo Fm facies associations (Figs. 5-6)

The Villar del Arzobispo Fm has been observed in both stratigraphic sections ACW and ACE (Fig. 3), where three facies associations have been distinguished:

C: Sandstone facies association

This facies association is observed in the middle part of the stratigraphic section ACW and in the lower part of the stratigraphic section ACE (Fig. 3) and is interbedded with marine carbonates of the peloidal and bioclastic facies (F3), the oolitic facies (F6) and locally with the rippled peloidal packstone facies (F2B). The association is formed by 0.40 to 5.50 m-thick sequences of very fine- to fine-grained sandstone (F5; Fig. 5A-D), commonly displaying parallel lamination (F5A) at the lower part and large-scale cross-bedding (F5B) at the upper part (Fig. 5C). Sandstone beds are occasionally formed by cross-bed sets that display tangential bottomsets and topsets (sigmoidal-like stratification *cf.* Mutti *et al.*, 1996). Paleocurrent measurements of these deposits indicate a predominant transport towards the northwest and a subordinate transport towards the southeast (Fig. 5B). Burrowing is occasionally observed in the upper part of the sandstone bodies. Sandstone is composed of quartz, feldspar, micritic intraclasts (50-100 µm), minor muscovite, biotite and scarce tourmaline. Bioclasts, carbonate intraclasts, and ooids may constitute up to 15% of the sediment in the lower part of the sandstone beds (Fig. 5D), but they are progressively less abundant upwards and bioclasts and ooids are even absent in the upper part of some sequences. Bioclasts consist of fragments of ostreids and other bivalves, echinoderms, serpulids, gastropods, small agglutinated forams, small miliolids, sponges, and plant remains. Carbonate intraclasts (200 µm-1,5 mm) have sub-angular to sub-rounded sections and show different carbonate textures (mudstone, wackestone of ooids, peloids and bioclasts).

Interpretation of facies association C

Based on the scarcity or even lack of fossils within the sandstones of this facies association, compared to the high proportion of marine fossils observed in the underlying and overlying marine carbonates, which, in turn, contain few siliciclastic grains, the sandstone facies association is interpreted as the result of siliciclastic discharges coming from the elevated areas of the continent and transported to the carbonate platform. After deposition in the carbonate platform, siliciclastic deposits would have been colonized by burrowers and/or reworked by marine currents. This is supported by paleocurrent data pointing to predominant transport directions

towards the northwest (indicating a transport towards the continent), because they coincide with the pathway of hurricanes during the Late Jurassic (Marsaglia and DeVries, 1983; Bádenas and Aurell, 2001a), which affected the storm-dominated carbonate ramp developed in other areas of the Iberian Basin (Bádenas and Aurell, 2001a; 2001b; 2004; 2010).

D: Oolitic and peloidal facies association

This facies association is observed in the lower-middle part of ACW stratigraphic section and in the lower part of ACE stratigraphic section (Fig. 3). It has been subdivided into two facies subassociations:

Facies subassociation D1. The *facies subassociation D1* overlies the *sandstone facies association C* in both stratigraphic sections (Fig. 3). It is formed by fining-upward sequences, 1.5-9 m thick, with flat or slightly irregular bases and tops (Fig. 6A). Sequences start with oolitic packstone-grainstone facies (F6), which gradually and rapidly changes upwards to peloidal packstone facies (F2A), rippled peloidal packstone facies (F2B) or mudstone facies (F7).

The oolitic packstone-grainstone facies (F6) is arranged in meter thick massive beds with occasional large-scale cross-bedding (Fig. 6A-B). The oolitic facies (F6) is composed of well-sorted ooids (50-200 µm; Fig. 6C), quartz grains, bioclasts, carbonate intraclasts, homogeneous fecal pellets (50-200 µm) and scarce oncoids. Ooid laminae have radial and micritic microstructures and their nuclei are formed by quartz grains, carbonate particles or fossil remains (Fig. 6C). Bioclasts are constituted of small and large agglutinated forams and miliolids and fragments of gastropods, echinoderms, bivalves and dasycladales. The foraminifers *Alveosepta* and *Nautiloculina* have been distinguished. Carbonate intraclasts show sub-rounded sections, submillimeter sizes (50-400 µm) and oolitic wackestone or packstone texture. The peloidal packstone facies (F2A and F2B) is similar to those described in the *facies associations A and B* (see above): they are formed by submillimetric fecal pellets and scarce fragments of gastropods and ostracods (F2A), or by fecal pellets, minor irregular micritic intraclasts, scarce small agglutinated forams and miliolids, scarce highly fragmented bivalves and echinoderms and scarce ooids, displaying wave and/or current ripples (F2B). The foraminifers *Kurnubia* aff. *palastiniensis* Henson and *Nautiloculina* have been observed. Mudstone facies (F7) is constituted of dense micrite, scarce small and large agglutinated forams, small miliolids, and fragments of bivalves, gastropods, brachiopods, and echinoderms.

The tops of the sequences are occasionally irregular and brecciated, displaying vertical dissolution structures that thin downwards (Fig. 6A). The breccia matrix and the infill of the vertical structures consist of very fine-grained sandstone.

Interpretation of facies subassociation D1

Deposits of the *facies subassociation D1* are interpreted as shallowing-upwards sequences similar to those described from ancient shallow carbonate platforms (e.g. Wilson,

1975; James, 1977; Enos, 1983, Caron *et al.*, 2005; Diedrich *et al.*, 2011; Sano *et al.*, 2012). These sequences were occasionally subaerial exposed, as suggested by the presence of irregular and brecciated tops and the thinning-downwards vertical structures, typically caused by edaphic processes (e.g. Alonso-Zarza and Wright, 2010). The good sorting, the packstone-grainstone texture, the presence of tractive structures and the fossil content of the oolitic facies (F6) indicate that these sequences were formed by the migration of oolitic shoals transported by tractive currents in the inner-carbonate platform, above the fair-weather wave-base. This interpretation is consistent with that given for the oolitic deposits of the Villar del Arzobipo Fm in the NW of Valencia province, which have been interpreted as oolitic shoals developed in the inner-carbonate platform (Mas and Alonso, 1981; Mas *et al.*, 1984). The nucleation of ooids was favored by the presence of abundant quartz grains in the platform, which were introduced by continental siliciclastic discharges (see *sandstone facies association C*). Protected areas were developed among the oolitic shoals, where invertebrate organisms produced abundant fecal pellets (peloidal packstone facies F2A, F2B), and where micrite accumulated under calm conditions (mudstone facies F7). This is similar to the shallow subtidal lagoon protected by oolitic shoals in the Great Bahama Bank in which mud and pellet facies-belts are complexly distributed (e.g. Purdy, 1963; Halley *et al.*, 1983; Reijmer *et al.*, 2009; Harris *et al.*, 2015). In fact, in the lagoon of the Great Bahama Bank the percentage of mud increases towards the coast of Andros Island (e.g. Bathurst, 1975; Kaczmarek *et al.,* 2010; Harris *et al.*, 2015), which according to Bathurst (1976), could be related to freshwater inputs from the swamps and channels of Andros Island into the areas next to the coast. Similarly, the distribution of the peloidal packstone facies and the mudstone facies in the *facies subassociation D1* could be related with freshwater inputs into the carbonate platform, as suggested by the fact that this facies subassociation overlies sandstone beds interpreted as the result of continental siliciclastic discharges (see *sandstone facies association C*). Furthermore, the fossil content of this association is less diverse than in *facies associations A and B*, a difference that could be explained by freshwater inputs, which would have produced a decrease in salinity, from normal marine to marine brackish waters.

Facies subassociation D2. The *facies subassociation D2* is observed above the *facies subassociation D1* in both stratigraphic sections (Fig. 3) and it is formed by 0.95-8 m thick sequences (Fig. 6D). The base of the sequences may be slightly irregular, including accumulation of angular and heterometric carbonate intraclasts (0.2-2 cm long; Fig. 6D-E). Sequences occasionally display irregular and brecciated tops, which show vertical dissolution structures, similar to those described in *facies subassociation D1* (Fig. 6F). Sequences start with oolitic packstone-grainstone facies (F6), which gradually changes upwards to bioclastic and peloidal packstone and packstone-grainstone facies (F8A). The bioclastic

and peloidal facies (F8A) is constituted of fecal pellets, micritic intraclasts and bioclasts (small and large agglutinated forams, small miliolids and trocholinids), which are more abundant than other fossil remains such as echinoderms, dasycladales, gastropods, ostreids and other bivalves (Fig. 6G). The foraminifers *Alveosepta*, *Nautiloculina* and *Labyrinthina mirabilis* (Fourcade and Neumann) have been distinguished, as well as dasycladacean algae *Salpingoporella granieri* Dieni & Radoicic (Fig. 6H-I), *Salpingoporella annulata* Carozzi (Fig. 6J-K) and *Holosporella* (Fig. 6L-M), (Dr. I. Bucur, personal communication). *Thalassinoides*-like traces are occasionally observed at the top of the beds. Locally, in the stratigraphic section ACE, in the upper part of this association, abundant quartz grains and charophytes have been observed together with gastropods and other mollusks, ostracods and scarce echinoderms.

In the stratigraphic section ACW, thickening and coarsening upwards siliciclastic sequences (up to 50 cm of thickness) are locally observed over these carbonate deposits (Fig. 6D, N). These siliciclastic sequences are constituted by thin layers of very fine-grained rippled sandstone (F11A) and marl (F9) at the base that change upwards to large-scale cross-bedded very fine- to fine-grained sandstone (F11B; Fig. 6N). Sandstone beds lack marine fossils and display burrowing (*Thalassinoides*-like traces) and wave ripples (F11A) at the top of the beds (Fig. 6N). Paleocurrent measurements of these deposits indicate a transport towards the east (Fig. 6D).

Interpretation of facies subassociation D2

Sequences of *facies subassociation D2* are interpreted as shallowing-upwards sequences deposited in a shallow carbonate platform, similar to those interpreted in *facies subassociation D1*. These sequences occasionally underwent periods of subaerial exposure, as occurred in *facies subassociation D1*. The shallowing-upwards sequences of the *facies subassociation D2* start with oolitic facies (F6) and gradually change upwards to bioclastic and peloidal facies (F8A). The textures and structures of these facies, together with their fossil content, indicate that they were deposited under agitated conditions in shallow areas of the carbonate platform and under marine brackish salinity waters. The abundance of quartz grains and the local presence of charophytes at the top of some sequences suggest that the shallow areas of the carbonate platform received occasional and local important freshwater and siliciclastic inputs from the continental areas.

Furthermore, the thickening and coarsening-upwards siliciclastic sequences, occasionally observed in the stratigraphic section ACW over the carbonate sequences of the *facies subassociation D2,* lack marine fossils and show a transport towards the east suggesting a continental provenance. Features of these siliciclastic sequences indicate that they were the result of siliciclastic discharges coming from the elevated areas of the continent and they were deposited as prograding lobes (*sensu* Ricci-Lucchi, 1975; Wright and Wilson, 1984; Zhang *et al.*, 2011) in shallow areas of the carbonate platform. These

deposits were reworked by wave currents and were affected by burrowers as it is evidenced by the wave ripples and the *Thalassinoides*-like traces observed at the tops of the sandstone beds.
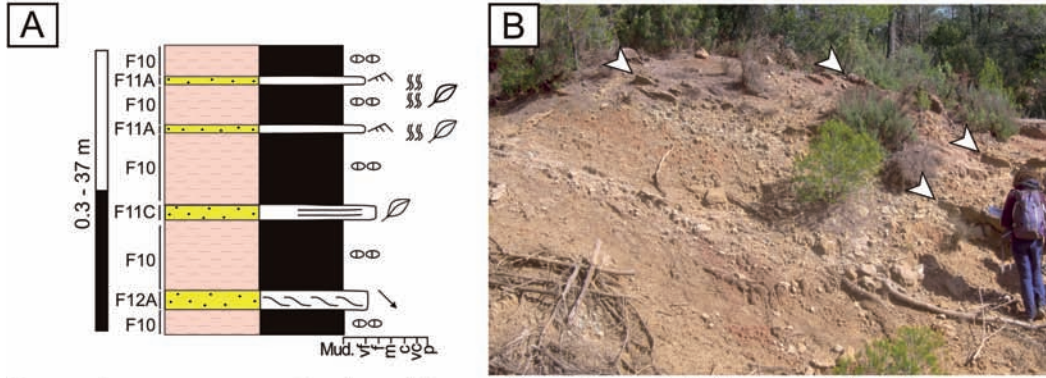
E: Marl-limestone-sandstone facies association

This facies association is observed in both stratigraphic sections, although it is poorly developed in the ACE section (Figs. 3, 6O). This association is constituted of marl (F9), interbedded with bioclastic and peloidal packstone and packstone-grainstone facies (F8A) and occasionally with sandstone (F11 and F12A). Marl (F9) layers are up to 20 m thick and show yellow and grey colors. The bioclastic and peloidal facies (F8A) is arranged in decimeter to meter thick massive or nodular beds, is poorly-sorted and is mainly formed by millimetric and submillimetric bioclasts (small and large agglutinated forams, small miliolids, trocholinids, and fragments of echinoderms, gastropods, serpulids, dasycladales, bivalves, ostracods, and solenoporacean red algae), fragments of ostreids up to 7 cm in size (Fig. 6P), quartz grains (10%), fecal pellets, carbonate intraclasts and scarce ooids and oncoids. The larger foraminiferal genus *Alveosepta* has been found in this unit (Fig. 3). Carbonate intraclasts are 50-700 µm in size and show mudstone and bioclast wackestone textures and peloidal and oolitic packstone textures. Moreover, *Rhizocorallium* burrowing is commonly observed in the bioclastic and peloidal facies (F8; Fig. 6P). Sandstone (F11 and F12A) beds are less abundant than limestone beds and occur as fine- to medium-grained decimeter- to meter- thick massive tabular levels with occasional large-scale cross-bedding (F11B), parallel lamination (F11C) or sigmoidal-like stratification (F12A; Fig. 6Q), and bioturbation. Paleocurrent measurements of these siliciclastic deposits indicate transport towards the east (Fig. 6O).

Interpretation of facies association E

This facies association, dominated by marl facies, directly overlies shallow marine carbonates (*facies association D;* Fig. 3) suggesting deposition in very shallow protected areas. Ramírez del Pozo found an ostracod association characteristic of brackish waters in marl of the middle to upper part of the ACW section (Assens *et al.,* 1973). Therefore, this marl facies is interpreted as deposited in a protected and brackish lagoon, which is consistent with previous interpretations of the Villar del Arzobispo Fm marl (Mas and Alonso, 1981; Mas *et al.*, 1984). Marl is commonly interbedded with bioclastic and peloidal facies (F8A). The poor sorting of the bioclastic and peloidal facies (F8A), their fossil content indicative of marine brackish salinities, and the presence of bioclasts of different sizes suggest that the marine components of this facies were transported into the lagoon by episodic currents (probably storms), from neighboring, shallow, marine brackish areas of the carbonate platform (*facies subassociation D2*). In general, it is a common feature of storm-dominated platforms that agitated events, such as storms, episodically
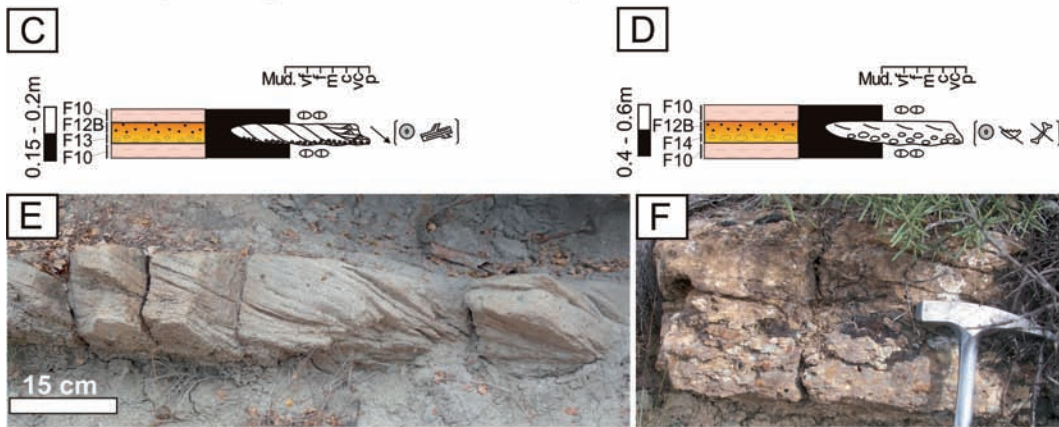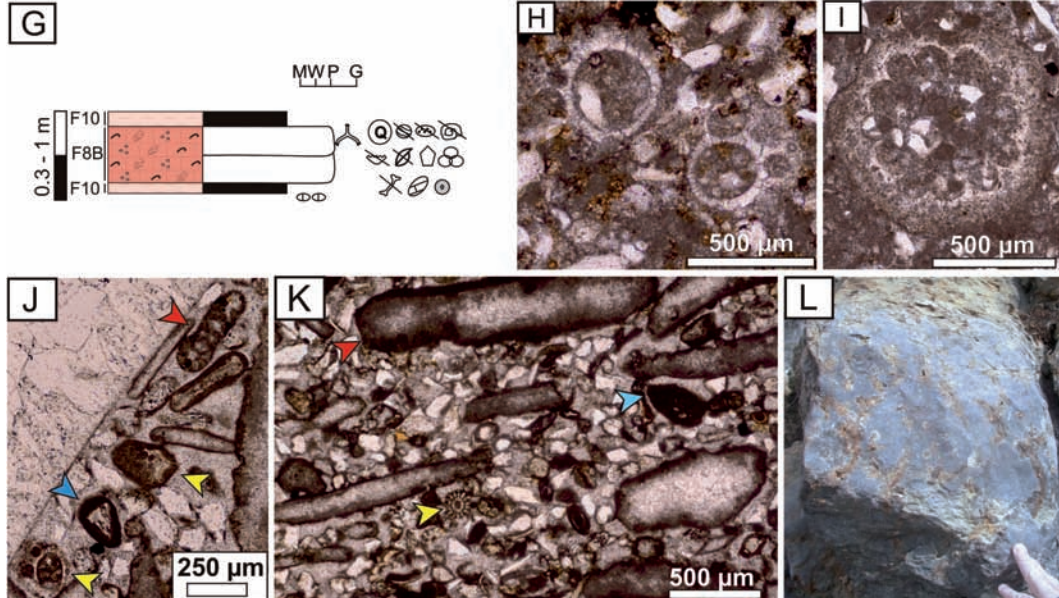
Fig. 7.- The Aldea de Cortés Fm facies associations. A-B) Siliciclastic mudstone-sandstone facies association F: A) Characteristic log of the siliciclastic mudstone-sandstone facies association F. See Fig. 3 for legend. B) Field photograph of the siliciclastic mudstone (F10) interbedded with thin layers of very fine- to fine-grained sandstone (F11) (arrows). C-F) Coarse- to very coarse-grained sandstone and conglomerate facies association G. C-D) Characteristic logs of the coarse- to very coarse-grained sandstone and conglomerate facies association G. See Fig. 3 for legend. E) Field photograph of the cross-bedded coarse- to very coarse-grained sandstone (F12B) and conglomerate (F13). Cross-bedding displays subhorizontal bottomsets and foresets (sigmoidal-like stratification). F) Field photograph of the massive clast-supported conglomerate (F14) changing upwards to coarse- to very coarse-grained sandstone (F12B). G-L) Limestone facies association H: G) Characteristic log of the limestone facies association H. See Fig. 3 for legend. H-I) TL micrograph of the bioclastic and peloidal facies (F8B) showing poorly preserved and fragmented charophytes. J) TL micrographs of the bioclastic and peloidal facies (F8B) with agglutinated forams (red arrow), fragments of charophytes (yellow arrows) and ooids (blue arrow). K) TL micrograph of the bioclastic facies (F8B) in which fragments of mollusks (red arrow), echinoderms (yellow arrow) and intraclasts (blue arrow) are observed. Note that the fragments of mollusks are rounded and oriented. L) Field photograph of the bioclastic and peloidal facies (F8B) displaying *Thalassinoides*-like traces filled by very fine-grained sand.

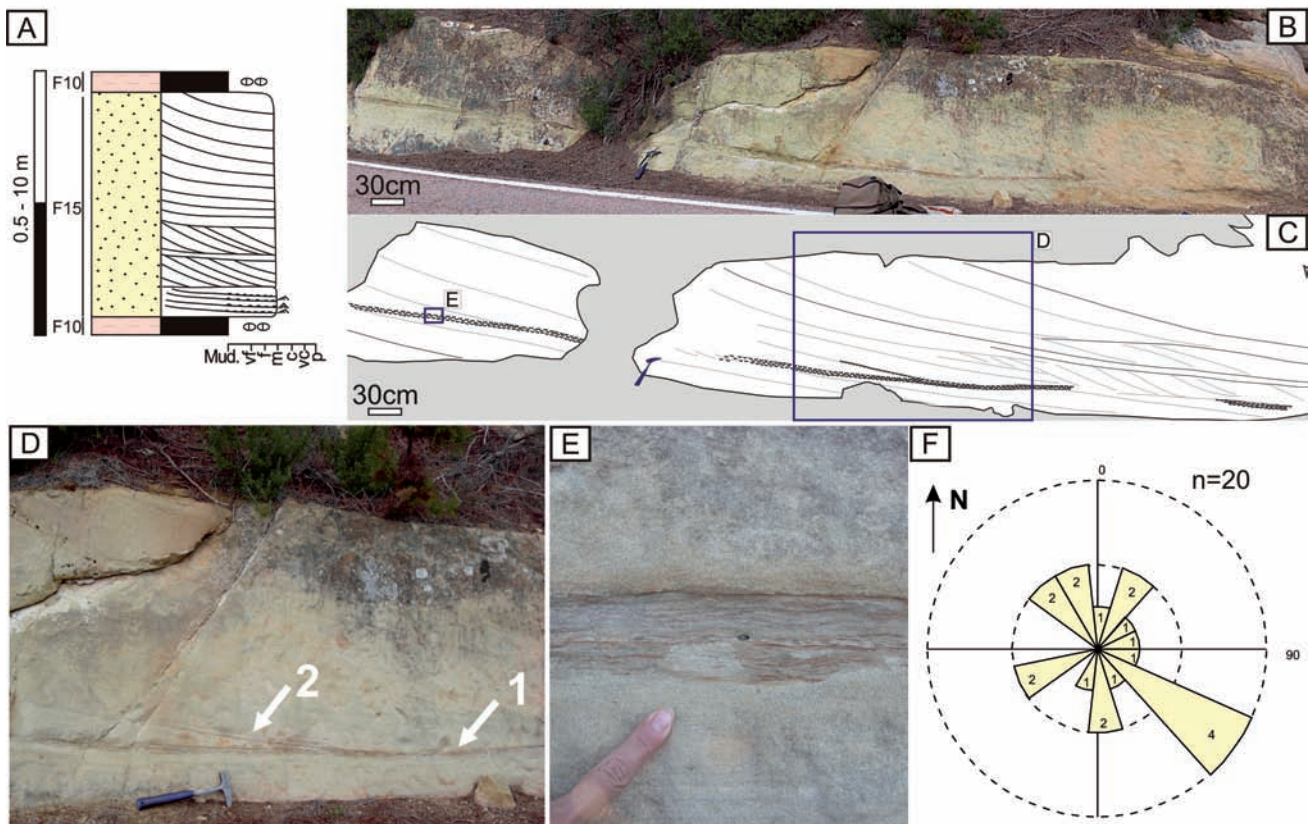## Large-scale cross-bedded sandstone facies association I

Fig. 8.- Large-scale cross-bedded sandstone facies association H of the Aldea de Cortés Fm. A) Characteristic log of the large-scale cross-bedded sandstone facies association H. See Fig. 3 for legend. B-C) Field photograph (B) and line drawing (C) of the fine-medium- to medium-grained, well- to very well-sorted sandstones (F11) displaying large-scale cross-bedding. Note the low angle foresets and the laterally continuous bottomsets of the thickest sets, and the high angle foresets of the thinner sets. D) The laterally continuous bottomsets (1) and, occasionally, the lower part of the foresets (2) are draped by mica flakes and plant remains. E) Detail of the bottomsets composed of rippled sandstone containing mica drapes and plant remains. F) Paleocurrent measurements, which indicate a principal transport towards the SE.

interrupt the calm conditions prevailing in the lagoonal areas (Aigner, 1985).

Regarding the scarce sandstone deposits interbedded with marl, their sedimentary structures (parallel lamination, large-scale cross-bedding, sigmoidal-like stratification), paleocurrents indicating a transport towards the east and the lack of fossil remains suggest that they arrived to the lagoon as siliciclastic discharges transported by tractive currents from the elevated continental areas. Moreover, the sigmoidal-like stratification that characterizes some sandstone beds is similar to that described by Mutti *et al.* (1996) and Turner and Tester (2006), and interpreted as the result of siliciclastic discharges entering ephemeral stagnant water bodies. Therefore, these features lead to interpret the siliciclastic deposits as the progradation of siliciclastic lobes into the lagoon.

4.3. Aldea de Cortés Fm facies associations (Figs. 7-8)

The Aldea de Cortés Fm is observed in both stratigraphic sections ACW and ACE (Fig.3). Four facies associations have been identified:

F: Siliciclastic mudstone-sandstone facies association

This facies association is observed in both stratigraphic sections ACW and ACE and it is interbedded with *facies associations G, H and I* (Fig. 3). It is formed by reddish and greenish siliciclastic mudstone (F10) commonly showing green mottling and carbonate nodules, interbedded with minor very fine- to fine- grained sandstone (F11 and F12A; see Fig. 7A-B), similar to those described in *facies association E. Ex situ* fragments of vertebrate remains (up to 9 cm in size) have been observed within siliciclastic mudstone (F10). Very fine- to fine-grained sandstone (F11) is arranged in decimeter thick beds (6-60 cm) with occasional current ripples (F11A), parallel lamination (F11C), millimetric and centimetric plant remains and bioturbation. Some fine-grained sandstone layers display sigmoidal-like stratification (F12A) characterized by foresets that thin and flat downdip and updip into tangential bottomsets and topsets. The foresets and the bottomsets are occasionally draped by mica flakes. Paleocurrent measurements of these deposits indicate transport toward the southeast (Fig. 7A).

Interpretation of facies association F

Reddish and greenish siliciclastic mudstone (F10) commonly displaying green mottling and carbonate nodules is interpreted as deposited in a flood plain, which underwent periodical subaerial exposure and development of paleosols (e.g. Freytet and Plaziat, 1982; Alonso-Zarza and Wright, 2010). Very fine- to fine-grained sandstone interbedded with siliciclastic mudstone is interpreted as the result of siliciclastic discharges coming from elevated continental areas, transported by tractive currents. The occasional sigmoidal-like stratification suggests, as in *facies association E*, that they were deposited as siliciclastic lobes in ephemeral stagnant water bodies (*cf.* Mutti *et al.*, 1996; Turner and Tester, 2006).

G: Coarse- to very coarse-grained sandstone and conglomerate facies association

This facies association is observed in both stratigraphic sections ACW and ACE (Fig. 3) and it is composed of coarse- to vey coarse-grained sandstone (F12B) and clast-supported conglomerate (F13, F14) occurring in fining upwards beds, which are interbedded with reddish and greenish siliciclastic mudstone (F10; see Fig. 7C-D). Cross-bedded conglomerate (F13) and coarse- to very coarse-grained sandstone (F12B) occur in fining-upwards beds with thicknesses of 15-20 cm and limited lateral extension of at least 4 m (Fig. C, E). The bases of the beds are commonly flat or slightly irregular. The lower part of these beds is made up of conglomerate composed of angular to sub-rounded carbonate clasts (0.2-1.6 cm in diameter) within a coarse to very coarse sandy matrix, and contain scarce fragments of plant remains (fragments of fossil trunks up to 5 cm in size) and very scarce ooids. This conglomerate changes gradually upwards to cross-bedded, coarse- to very coarse-grained, poorly-sorted sandstone with scatter carbonate pebbles. This sandstone displays tangential bottomsets and topsets (sigmoidal-like stratification; see Fig. 7C, E). Paleocurrent measurements of these deposits indicate a transport towards the southeast (Fig. 7C).

Other fining-upwards beds (40-60 cm of thickness) are composed of massive clast-supported conglomerate (F14), which change upwards to cross-bedded coarse- to very coarse-grained sandstone (F12B). These beds show limited lateral extension (up to 3 m) and slightly irregular bases (Fig. 7D, F). The lower part of these beds is formed by poorly- to very poorly-sorted massive clast-supported conglomerate, which is composed of angular to sub-rounded carbonate clasts and scarce quartzite clasts (0.2-5 cm in diameter) within a fine- to medium-grained sandy matrix, and contain very scarce fragments of ostreids, ooids, vertebrate remains and plant remains (fragments of fossil trunks up to 12 cm in size; Fig. 7D). This conglomerate changes gradually upwards to coarse- to very coarse-grained sandstone (F12B) occasionally displaying large-scale cross-bedding (Fig. 7D, F).

Interpretation of facies association G

Conglomerate and coarse- to very coarse-grained sandstone occurring in fining-upwards beds and interbedded with siliciclastic mudstone are interpreted as the result of clastic discharges transported by ephemeral currents and deposited in a flood plain, which was periodically subaerially exposed and affected by edaphic processes. The sigmoidal-like stratification observed in some coarse- to very coarse-grained sandstone suggests that some of these clastic discharges were deposited as lobes in ephemeral stagnant water bodies in the flood plain (*cf.* Mutti *et al.*, 1996; Turner and Tester, 2006), as occurs in the lagoon and flood plain facies associations (*facies associations E* and *F*). Moreover, paleocurrent measurements indicating a transport towards the southeast suggest that these clastic discharges came from elevated continental areas. In addition, the presence of very scarce ooids and fragments of ostreids within the facies of this association suggests that deposition took place in coastal areas as it is discussed later in the *limestone facies association H* (see below).

H: Limestone facies association

This facies association is observed in both stratigraphic sections ACW and ACE (Fig. 3). It is composed of bioclastic and peloidal packstone and packstone-grainstone facies (F8B; Fig. 7G-L) interbedded with reddish and greenish siliciclastic mudstone (F10), which often shows green mottling and carbonate nodules (Fig. 7G). The bioclastic and peloidal facies (F8B) is arranged in decimeter to meter thick massive beds (up to 1 m thick), and is composed of poorly- to very poorly-sorted bioclasts (fragments of charophytes, ostracods, gastropods, ostreids and other bivalves up to 4 cm in size, and scarce echinoderms, small agglutinated forams, small miliolids, and millimeter-scale vertebrate remains; Fig. 7H-K), sub-angular quartz grains (20-25%), fecal pellets (50 to 100 µm), intraclasts, and scarce ooids (Fig. 7J). Intraclasts are sub-rounded to sub-angular, show submillimeter to millimeter sizes (50 µm-1.6 mm), and have different textures: mudstone, wackestone and packstone of bioclasts, peloids and quartz grains. Some bioclastic and peloidal layers show a grainstone texture in which fragments of bivalves are rounded to subrounded and are oriented parallel to the bedding (Fig. 7K). *Thalassinoides*-like traces are occasionally observed at the top of the beds (Fig. 7L).

Interpretation of facies association H

This facies association is formed by limestone interbedded with reddish and greenish siliciclastic mudstone with mottling and carbonate nodules suggesting frequent subaerial exposure and paleosol development (as interpreted for *facies associations F and G*). Limestone contains ooids and fossil remains of marine affinity (ostreids, forams and echinoderms), which are similar to those described in the lagoon facies association (*facies association E*) but are less abundant. Moreover, limestone of this association contains abun-

dant quartz grains and fossils indicative of freshwater environments (charophytes). Therefore, the fossil content of this limestone indicates a mixture of water sources: seawater from shallow marine areas and freshwater from continental areas. The components of limestone are also poorly- to very poorly-sorted, suggesting that they were transported by episodic events, such as storms and/or flooding. During these events, marine bioclasts and ooids may have been transported from neighboring areas with marine waters, whereas charophytes, which are commonly fragmented, and quartz grains may have been transported from freshwater environments. As a whole, this association is interpreted as a low gradient coastal plain that could have been easily flooded, but also periodically desiccated allowing the development of very shallow and relatively ephemeral water bodies separated by vegetated areas. Locally, some of these water bodies could have been more stable and remained longer in the coastal plain, allowing continuous agitation by currents, probably waves, which would explain the abrasion and rounding of bioclasts, the orientation of elongated bioclasts, and the grainstone texture observed in some layers. Furthermore, some of these shallow and more stable water bodies could have been colonized by marine burrowers, as indicated by the *Thalassinoides*-like traces at the top of some beds.

I: Large-scale cross-bedded sandstone facies association

This facies association is observed in both stratigraphic sections ACW and ACE (Fig. 3). It is formed by fine- to medium-grained, well- to very well-sorted, cross-bedded sandstone (F15), which is interbedded with reddish and greenish mottled siliciclastic mudstone (F10; Fig. 8A). Sandstone bodies are arranged in decimeter to meter thick beds (up to 10 m in thickness) of great lateral continuity (from 100 m to, at least, 300 m wide; Fig. 8B-C), and show flat or slightly irregular bases and flat tops. Sandstone bodies display large-scale cross-bedding (Fig. 8A-B) and may show oblique erosion surfaces separating sets of cross-strata producing wedge-shaped sets (F15A). Towards the lower part of the sandstone bodies, cross-bedded sets are commonly thinner (less than 60 cm; see Fig. 8A-C) and display high angle (up to 30º) foresets, short lateral extension and reactivation surfaces (F15A). Cross-bedded sets commonly become thicker upwards (up to 2.20 m; see Fig. 8A-C), displaying low angle foresets (less than 15º), laterally continuous bottomsets and reactivation surfaces (F15A). The bottomsets and, occasionally, the lower part of the foresets of low angle sets may be draped by thin layers of plant remains and mica flakes (F15A; Fig. 8D-E). Locally, current and wave ripples, also draped by plant remains and mica flakes, are observed at the bottomsets (F15B; Fig. 8E). Sub-rounded to angular muddy soft pebbles (0.2-3 cm) are present in some foresets. Paleocurrent measurements of these deposits indicate main transport towards the SE (Fig. 8F).

Interpretation of facies association I

Cross-bedded sandstone bodies (F15) show several sedimentary structures (reactivation surfaces, current and wave ripples at the bottomsets, and mica flakes and plant remains draping the bottomsets and occasionally the lower part of the foresets), which are commonly interpreted as tidal in origin (e.g. Nio and Yang, 1991; Pontén and Plink-Bjorklund, 2009; Martinius and Van den Berg, 2011). In fact, these sandstone bodies have been previously interpreted as subtidal bars developed in a tide-influenced deltaic plain (Mas 1981; Mas *et al.*, 2004). Nevertheless, if they had been deposited as subtidal bars it would be expected that they contained marine fossils, as all the facies interpreted as deposited in marine settings (see *facies associations A, B, D, E* and *F*). Moreover, if they had been deposited as subtidal bars, it would also be expected that they were laterally and vertically associated with facies containing tidal structures, such as flaser, wavy and lenticular bedding (e.g. Reineck and Wunderlich, 1968; Dalrymple, 2010), which have not been observed in the study area. On the contrary, the cross-bedded sandstone bodies (F15) are interbedded with reddish siliciclastic mudstone (F10) with common edaphic features, which do not contain any marine fossils and show little evidence of tidal influence. Therefore, a subtidal origin for the sandstone bodies may be questioned, although minor tidal influence is not discarded.

Furthermore, features of the cross-bedded sandstone bodies (F15), such as great lateral continuity, thick sets, fine-medium- to medium-grain size, good to very good grain-sorting, low angle foresets occurring in sets of great thickness, high angle foresets, reactivation surfaces, wedge-shaped sets and even muddy soft pebbles within the sandy foresets, have been described by many authors as common features of aeolian dunes in modern and ancient examples (e.g. Kocurek, 1981; Hunter *et al.*, 1983; Langford and Chan, 1989; Clemmensen *et al.*, 2001; Mountney, 2006; Rodríguez-López *et al.*, 2008). Moreover, the presence of current and wave ripples at the bottomsets, and the presence of mica flakes and plant remains in the bottomsets and in the lower part of the foresets are common features in wet aeolian interdunes, which develop as the result of a rapid rise of the water-table due to occasional fluvial inundations, ephemeral flash flooding from rainfall events, or in coastal settings by spring tides, storms, or periods of low air pressure (e.g. Kocurek, 1981; Langford, 1989; Langford and Chan, 1989; Mountney, 2006; Rodríguez-López *et al.*, 2008; Tripaldi and Limarino, 2008).

Therefore, all these features suggest that the cross-bedded sandstones bodies of this association were aeolian in origin, locally affected by ephemeral water courses. The aeolian deposits could have been affected by tides, as reported in other modern and ancient environments with tidal-aeolian interactions (e.g. Fryberger *et al.*, 1990; Rodríguez-López *et al.*, 2012).
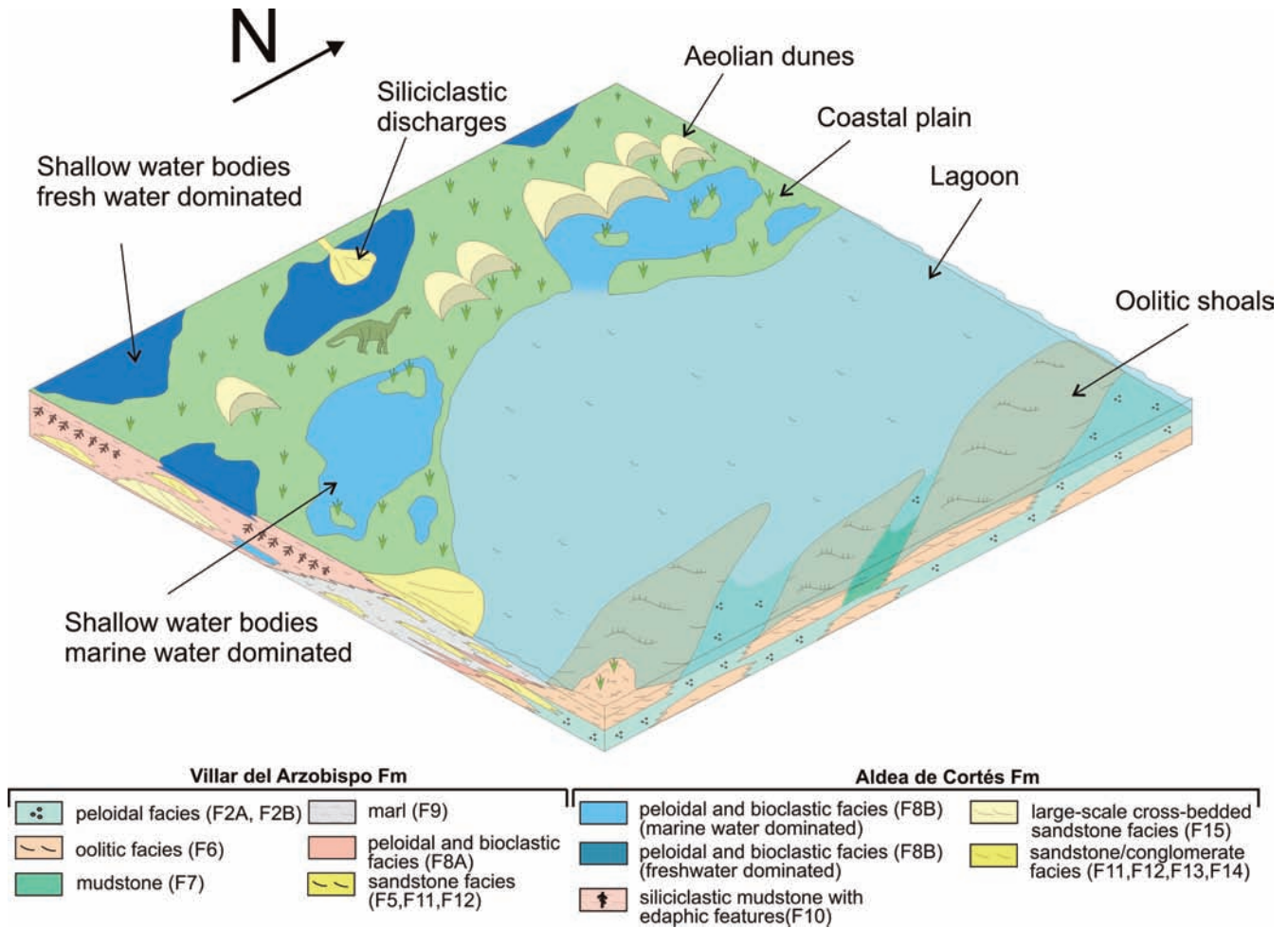
Fig. 9.- Idealized reconstruction of the different subenvironments where the Villar del Arzobispo and Aldea de Cortés Fms were deposited in the Benagéber area during the Late Jurassic-Early Cretaceous times.

5. Depositional system and evolution of the studied units in the Benagéber area

The vertical arrangement of all the facies associations from the three studied units (Fig. 3) indicates the gradual shallowing upwards of a carbonate platform that progressively evolved into a complex coastal system.

The Higueruelas Fm started to develop in a mid-carbonate platform under the fair-weather wave base and above the storm wave base, where subtidal oncolitic shoals migrated by the action of storm currents (F1). These shoals protected calm areas where invertebrate organisms produced abundant fecal pellets (F2A; *facies subassociation A1*). Upwards, oncolitic shoals progressively developed in the inner-carbonate platform, above the fair-weather wave base and in normal marine salinity waters, as indicated by the continuous concentric laminae of oncoid cortices (F3) and the wave ripples observed in the rippled peloidal deposits (F2B; *facies subassociation A2*). Gradually, peloidal and bioclastic shoals (F4) migrated in the inner-carbonate platform, where oncoid development was progressively decreasing as it is indicated by the thickness reduction of oncoid cortices.

The Higueruelas Fm transitionally changed upwards to the Villar del Arzobispo Fm when siliciclastic inputs from continental areas started to occur. Siliciclastic discharges were related to the tectonic activity associated with the beginning of the Late Jurassic-Early Cretaceous *rifting* phase (Aurell *et al.*, 1994; Mas *et al.*, 2004) and they implied several and rapid changes in the sedimentation and configuration of the platform. The arrival of siliciclastic discharges to the platform (*facies association C*), probably coming from the Iberian and Valencian Massifs located westwards and northwards of the basin, respectively (Mas *et al.*, 2004), favored the nucleation of ooids, whereas the oncoid production ceased. Storms probably reworked these continental siliciclastic discharges as suggested by predominant transport directions towards the NW (see paleocurrent data in Fig. 5B; *facies association C*), which was the pathway of hurricanes in the Late Jurassic (Marsaglia and DeVries, 1983; Bádenas and Aurell, 2001a). Ooids migrated in shoals and protected a shallow lagoon (Fig. 9), in which fecal pellets were produced by invertebrate organisms and micrite accumulated (*facies subassociation D1*). Progressively, sedimentation took place in shallower and inner areas of the platform that underwent common

subaerial exposure. These areas were affected by siliciclastic discharges and freshwater inputs from continental areas, with a general transport towards the east, which caused a progressive decrease in salinity and the consequent change in biota (*facies subassociation D2*). During the last stages of the Villar del Arzobispo Fm, sedimentation took place in a shallow, brackish and protected lagoon affected by the arrival of neighboring marine carbonate deposits transported by storms and also by the arrival of continental siliciclastic discharges, which also show a sense of transport with paleocurrents towards the east (*facies association E*).

The Aldea de Cortés Fm deposits have been interpreted in this study as developed in a low gradient complex coastal plain where multifaceted environments have been recognized (Fig. 9): i) flood plain areas that were periodically flooded and desiccated, with significant development of vegetation (*facies association F*); ii) shallow and ephemeral water bodies influenced by both fresh and marine waters, as it is suggested by the presence of carbonate deposits containing fossils of freshwater affinity (charophytes) and quartz grains, but also fossils of marine affinity (ostreids, scarce forams, echinoderms, and ooids), which would have been transported from the continent and from marine areas, respectively, during storm or flooding episodes (*facies association H*); iii) siliciclastic discharges coming from elevated continental areas and transported by ephemeral currents (*facies association F and G*); and, iv) aeolian dunes and interdunes (*facies association I*).

All these features suggest that sedimentation of the Aldea de Cortés Fm took place in a "coastal wetland" (*sensu* Suarez-Gonzalez *et al.*, 2015), because it includes numerous sedimentological features that characterize this type of depositional system: shallow-water facies containing both continental and marine fossils, common subaerial exposure, edaphic features, and complex distribution of interbedded continental, transitional, and marine deposits. Mas (1981), Mas and Alonso (1981), and Mas *et al.* (1982) and interpreted the unit, in the study area, as deposited in a lagoon surrounded by a tidal flat environment which, in turn, was surrounded by a fluvial deltaic plain. Specifically, these authors interpreted the carbonate deposits of this unit as developed in a lagoon. However, these carbonate deposits contain abundant charophytes and marine fossils and occur interbedded with siliciclastic mudstone with common edaphic features. These features indicate deposition in shallow to very shallow water bodies in a low gradient and vegetated coastal plain, which

was easily flooded by both fresh and marine waters rather than in a lagoon. In addition, these authors interpreted that the lagoon was surrounded by tidal flats (Mas, 1981; Mas and Alonso, 1981; Mas *et al.* 1982). In this sense, although local tidal influence in the aeolian deposits is not excluded (*facies association I*), other typical facies associations of tide-dominated environments, such as tidal channels, tidal bars or sand flats (e.g. Dalrymple, 2010), have not been observed. Moreover, these authors also interpreted that fluvial deltaic plains surrounded the tidal flat-lagoon environments (Mas, 1981; Mas *et al.* 1982; Mas and Alonso, 1981). Deposition in a delta system would require the presence of distributary channel deposits (e.g. Bhattacharya, 2006; 2010) and these have not been observed. Nevertheless, it should not be discarded that the coastal wetland could have been part of a larger deltaic system, as reported in several modern and ancient examples (e.g. Calder et al, 2006; Rygel, *et al.*, 2006; Sasser *et al.*, 2009; Wolanski *et al.*, 2009; Woodroffe and Davies, 2009).

Concerning the contact between the Villar del Arzobispo and the Aldea de Cortés Fms, previous studies have interpreted it as an unconformity (Fig. 2A; Mas, 1981; Mas *et al.*, 1982; Mas and Alonso, 1981; Mas *et al.*, 1984; Aurell *et al.,* 1994; Mas *et al.*, 2004). However, the detail study of both units strongly suggests a gradual transition between them, which thus would have been laterally related, because no evidence of an unconformity has been observed, and because the sedimentological and paleontological features observed in the upper deposits of the Villar del Arzobispo Fm (*facies associations E*) are similar to those observed in the Aldea de Cortés Fm (*facies association H*), although with increasing freshwater input in the last.

In sum, the sedimentary succession studied here corresponded to a complex and dynamic system formed by a mosaic of diverse shallow-marine and coastal facies (*cf.* Wilkinson and Drummond, 2004; Suarez-Gonzalez *et al.*, 2015), as it has been reported in numerous modern systems, such as Bahamas (e.g. Bathurst, 1975; Reijmer *et al.*, 2009; Kaczmareck *et al.*, 2010; Harris *et al.*, 2015), Persian Gulf (e.g. Wagner and Van der Togt, 1973; Wilkinson and Drummond, 2004), Antigua (e.g. Wilkinson and Drummond, 2004) and Gulf of Batabano (e.g. Daetwyler and Kidwell, 1959; Hoskins, 1964). These modern environments show a wide range of different sediment types, which are commonly complexly distributed due to the combination of multiple factors such as differences in tectonics, subsidence rate, salinity variations, intensity of currents, water turbulence, mean water

---

Fig. 10.- (next page) *Alveosepta personata* (Tobler). A) Oblique-tangential section of a large specimen (probable a B-form) showing the structured septa and the subepidermal "alveoles" in the lateral chamber walls. Sample: Ac1035. B, I-K) Slightly oblique sections cut almost parallel to the equatorial section of A-forms. All of them show the structured septa and the supplementary foramina developed between the long beams. In the tangential cuts the subepidermal "alveoles" are visible in the lateral chamber walls. Note the peneropliform style growth of the last adult chambers and the empty chamber lumina. Samples: ACE013, Ac1027. C) Subaxial section showing two spiral whorls. B-form?. Sample: Ac1035. D-F) Equatorial sections (E and F are a little oblique) of A-forms showing the complex embryo. In the last chambers of the specimen D the main foramen can be appreciated. Samples: Ac1035, ACE013. G) Subaxial section far from the axial section showing the supplementary foramina crossing the septa between the exoskeleton structures. In the lower part of the picture the lateral chamber wall cutted tangentially allows to observe the regularity of the "alveoles". B-form?. Sample: ACE014. H) Oblique section showing the chambers of the last whorl. Probably a B-form. Sample: Ac1035.
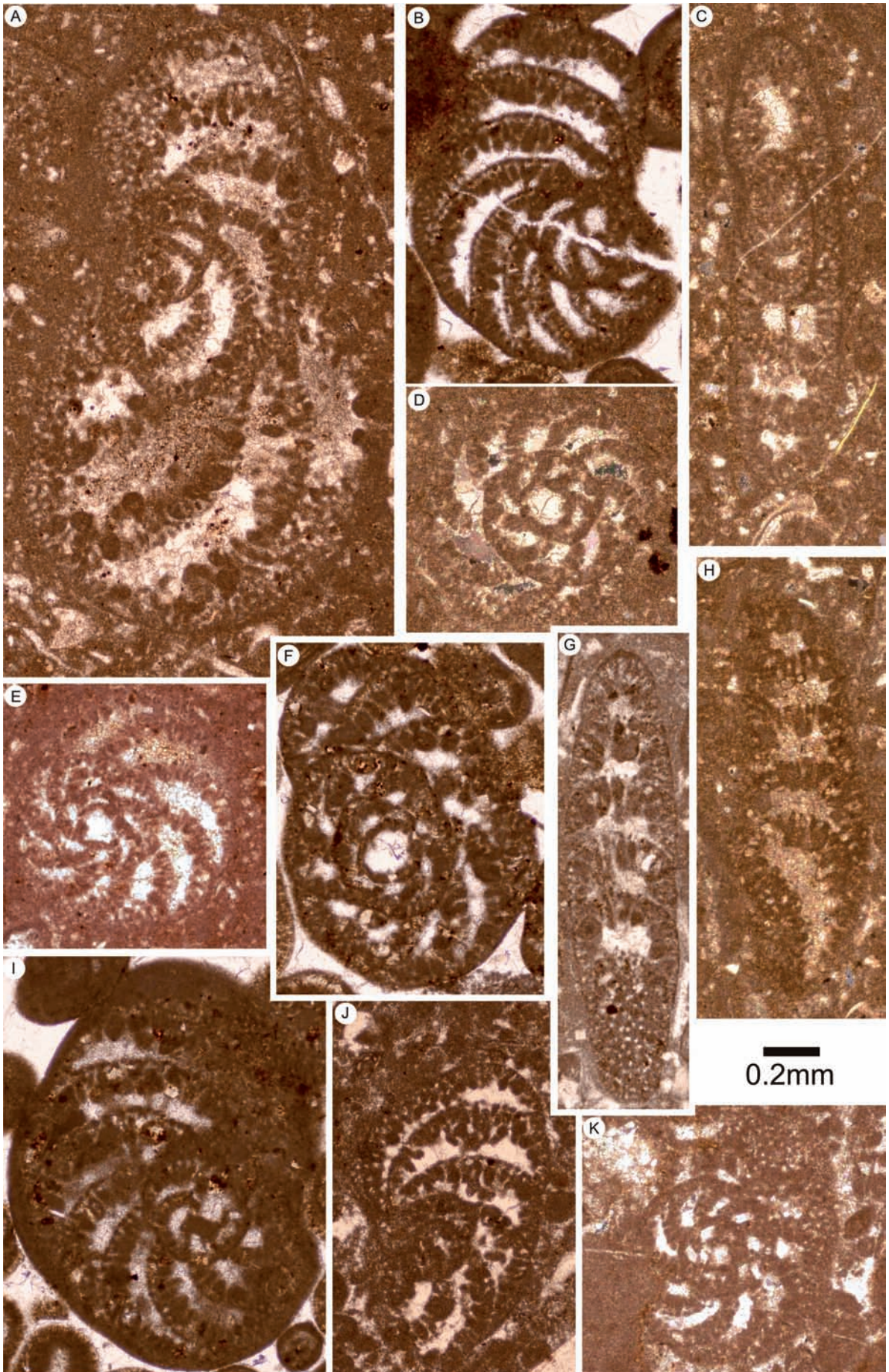
depth, nutrients availability, and climatic conditions, among others, as it is explained in the articles previously mentioned.

6. Remarks on larger foraminifera. Revisiting the age of the studied units at the Benagéber area.

The detailed sedimentological study presented in this work has also brought to light new and interesting paleontological data that have important implications for the poorly constrained age of the studied units. In the lower part of the Villar del Arzobispo Fm several carbonate beds yield abundant sections of a larger foraminifer that has been attributed to the genus *Alveosepta* Hottinger (type species: *Cyclammina jaccardi* Schrodt, 1894). It is characterized by its finely agglutinated, compressed shell with strong dimorphism. In the adult growth stages, the chambers are planispiral arranged in both A- and B- generations, but in the juvenile stages of B-forms they are streptospiral. The external wall presents exoskeleton elements constituted by beams and rafters forming a subepidermal network covered by a fine epidermis, which in contrast with other contemporaneous genera like *Pseudocyclammina* Yabe and Hanzawa, prolong to the septa (structured septa in Hottinger, 1967). The main foramina are large and placed at the base of the septa, but some small foramina are irregularly distributed in the median part of the septa interrupting the epidermis. *Alveosepta* lacks endoskeleton. The age attributed to the genus *Alveosepta* is late Oxfordian-Kimmeridgian (Bassoullet, 1997; Loeblich and Tappan, 1987).

The specimens found in the Villar del Arzobispo Formation are attributed in this paper to *A. personata* (Tobler, 1928), a species considered synonymous of *A. jaccardi* by Maync (1960), but with a looser spire than *A. jaccardi* type (Fig. 10). After Hottinger (1967) and Bassoullet (1997) *A. personata*, which was described as *A. jaccardi* from the Suisse Jura, seems to characterize a younger stratigraphical level than *A. jaccardi* (see Fig. 40 in Hottinger, 1967). However, further detailed studies are needed in continuous series with abundant larger foraminifer populations to prove each replacement in time. If the specimens mentioned by Viallard (1973) and Ramirez del Pozo (Assens *et al.*, 1973) in the underlying deposits of the Higueruelas Fm are the true *A. jaccardi* or not remains without answer, because no good figurations are given by these authors.

The specimens of *A. personata* are represented mainly by A-forms, but B-forms are also present. The A-forms consists of a complex embryo followed by at least two whorls of planispiral chambers; the first whorl has 7-8 chambers; the second has 10-11 and the incomplete third whorl about 2-3 chambers. These measurements coincide with those given by Hottinger (1967) from *A. personata* from the Jura and from Morocco (see plates 15 and 16 in Hottinger, 1967, for comparison).

The Villar del Arzobispo Fm has been attributed to an age of Late Tithonian-Middle Berriasian by Aurell *et al.* (1994)

and Mas *et al.* (2004). However, the paleontological data obtained in this study indicate that at least the age of the lower part of the Villar del Arzobispo Fm is Kimmeridgian, while the age of the upper part may be Tithonian (since Ramírez del Pozo mentioned *Anchispirocyclina* in Assens *et al.*, 1973), although the typical tithonian fauna has not been found (Fig. 2B). Thus, the age of the underlying unit, the Higueruelas Fm, should not be younger than Kimmeridgian (Fig. 2B), instead of Tithonian, as assigned by Aurell *et al.* (1994).

The Aldea de Cortés Fm has previously been attributed to a Valanginian-Hauterivian age without paleontological justification because it lacks paleontological content which allows an accurate dating of the unit (Mas, 1981; Mas *et al.*, 1982; 2004; Mas and Alonso, 1981). However, the beginning of the deposition of the Aldea de Cortés Fm should be attributed to an age not younger than Tithonian, at least in the area of Benagéber, as the contact between the Villar del Arzobispo and the Aldea de Cortés Fms has been revealed to be transitional and not unconformable, as suggested in previous studies.

The stratigraphical and sedimentological contributions provided in this work involve important chronostratigraphical and paleogeographical implications, which would affect the correct dating of the beginning of the South Iberian Basin sedimentary infill. In this sense, the Kimmeridgian age of the Villar del Arzobispo Fm fits better with the Kimmeridgian age proposed by Salas *et al.* (2001) for the climax of the Late Jurassic *rifting* stage in the Iberian Basin; in fact this *rifting* stage led to significant increasing of siliciclastic inputs into the carbonate platforms, as occurred in the Villar del Arzobispo Fm. Moreover, these new data encourage reviewing the nomenclature and stratigraphic framework of the Villar del Arzobispo and Aldea de Cortés Fms, as well as the previously proposed stratigraphic correlations between the studied units and those deposited in adjacent areas of the Iberian Basin, such as in the Maestrat Basin (Salas *et al.*, 2001; Mas *et al.*, 2004).

These implications would also have repercussions on the dating of the dinosaur sites discovered in the Villar del Arzobispo Fm in this Basin (e.g. Santisteban *et al.*, 2002; Suñer *et al.*, 2008; Santisteban *et al.*, 2008; Pereda *et al.*, 2009; Royo-Torres *et al.*, 2009; Cobos *et al.*, 2010), with an age range Kimmeridgian-Tithonian, and of the historical sites from the Benagéber area included here in the Aldea de Cortés Fm. In this regard Trullenque (1915) announced the presence of reptilian bones and assigned them to the Jurassic. Later, Royo y Gómez and other authors considered other dinosaur remains of Benagéber as "wealdian" (see Royo y Gómez 1926a; 1926b; Pérez-García *et al.*, 2009), but finally, in 1927, Royo y Gómez reassigned the dinosaur remains to the "Purbeck" instead of the "Weald". Therefore, the data provided in the present work corroborate the results given by Royo y Gómez in 1927 because, as discussed in this article, the Aldea de Cortés Fm may be considered part of the regressive trend

(Aurell *et al.*, 1994) of the Late Jurassic-Early Cretaceous cycle; thus, facies of the Aldea de Cortés Fm seem to be correlatable with siliciclastic-dominated deposits of the middle and upper part of the Villar del Arzobispo Fm in surrounding areas of the South Iberan Basin, such as its type section (Mas *et al.*, 1984) and the Riodeva area (Luque *et al.*, 2005; Campos-Soto *et al.*, 2015).

7. Conclusions

The detail study of the Upper Jurassic-Lower Cretaceous deposits of the Benagéber area (South Iberian Basin, E Spain) has led to new sedimentological and chronostratigraphical interpretations:

- The Higueruelas and Villar del Arzobispo Fms were deposited in a prograding carbonate platform affected by storms with an upwards decrease in oncoid development and increase in siliciclastic discharges from continental areas. In turn, the carbonate platform progressively evolved into a coastal wetland system (Aldea de Cortés Fm) affected by the arrival of continental siliciclastic discharges and migration of aeolian dunes.

- The transition between the Higueruelas and the Villar del Arzobispo Fms was gradual but took place rapidly because the arrival of the continental siliciclastic discharges ceased the oncoid production in the carbonate platform. Then, deposition of oolitic shoals and lagoonal marl took place in the inner platform-lagoon and salinities decreased, contributing to a progressive change in the biota.

- The transition between the Villar del Arzobispo and the Aldea de Cortés Fms has been reinterpreted here as gradual, instead of unconformable as interpreted before, due to several evidences: 1) the arrangement of the facies associations of both units shows a gradual transition between them; 2) the fossil remains observed in the upper part of the Villar del Arzobispo Fm are similar to those of the Aldea de Cortés Fm, both indicating influence of both fresh and marine waters, although with increasing freshwater input in the latter, in accordance with the overall Late Jurassic-Early Cretaceous prograding trend. Thus, the Aldea de Cortés Fm should be considered part of the Late Jurassic-Early Cretaceous cycle.

- The presence of the benthic foraminifer *Alveosepta personata* in the lower part of the Villar del Arzobispo Fm suggests that the lower part of the unit should be assigned to the Kimmeridgian in the Benagéber area, instead of Late Tithonian-Middle Berriasian (Aurell *et al.*, 1994; Mas *et al.*, 2004). Consequently, the age of the Higueruelas Fm should not be younger than Kimmeridgian, instead of Tithonian (Aurell *et al.*, 1994), and the beginning of the deposition of the Aldea de Cortés Fm should be attributed to an age not younger than Tithonian, instead of Valanginian (e.g. Mas, 1981; Mas and Alonso, 1981; Mas *et al.*, 1982).

- These new data encourage revising the previously proposed stratigraphic correlations between the studied units and those deposited in adjacent areas of the Iberian Basin.

References

Aigner, T. (1985): *Storm Depositional Systems-Dynamic Stratigraphy in Modern and Ancient Shallow Marine Sequences*. Springer, Berlin, 174 p.

Alonso-Zarza, A.M., Wright, V.P. (2010): Palustrine carbonates. In: A.M. Alonso-Zarza, L.H. Tanner (eds.), *Carbonates in Continental Settings: Geochemistry, Diagenesis and Applications*. Developments in Sedimentology 61, Elsevier, Amsterdam, pp. 103-132. doi: 10.1016/S0070-4571(09)06202-5.

Assens, J., Ramírez del Pozo, J., Giannini, G., Riba, O., Vilena, J., Reguant, S. (1973): Hoja geológica num. 666 (Chelva). *Mapa Geológico de España E. 1:50.000*. Segunda serie, I.G.M.E., Madrid.

Aurell, M. (1990): *El Jurásico Superior de la Cordillera Ibérica Central (provincias de Zaragoza y Teruel). Análisis de cuenca*. Tesis Doctoral, Universidad de Zaragoza, Zaragoza, 510 p.

Aurell, M., Bosence, D., Waltham, D. (1995): Carbonate ramp depositional systems from a late Jurassic epeiric platform (Iberian Basin, Spain): a combined computer modeling and outcrop analysis. *Sedimentology* 42, 75-94. doi: 10.1111/j.1365-3091.1995.tb01272.x

Aurell, M., Mas, R., Meléndez, A., Salas, R. (1994): El tránsito Jurasico-Cretácico en la Cordillera Ibérica: relación tectónica-sedimentación y evolución paleogeográfica. *Cuadernos de Geología Ibérica* 18, 369-396.

Aurell, M. Bádenas, B., Bello, J., Delvene, G., Meléndez, G., Pérez-Urresti, I., Ramajo, J. (1999): El Calloviense y el Jurásico Superior en la Cordillera Ibérica Noroccidental y la Zona de Enlace con la Cordillera Costero-Catalana, en los sectores de Sierra de Arcos, Calanda y Xert-Paüls. *Cuadernos de Geología Ibérica* 25, 73-110.

Aurell, M., Meléndez, G., Olóriz, F., Bádenas, B., Caracuel, J. E., García-Ramos, J. C., Goy, A., Linares, A., Quesada, S., Robles, S., Rodríguez-Tovar, F. J., Rosales, I., Sandoval, J., Suárez de Centi, C., Tavera, J. M., Valenzuela, M. (2002): Jurassic. In: W. Gibbons and T. Moreno (eds.), *The Geology of Spain*. Geological Society, London, pp. 213-254.

Bádenas, B. (1999): *La sedimentación en las rampas carbonatadas del Kimmeridgiense en las cuencas del Este de la Placa Ibérica*. Tesis Doctoral, Universidad de Zaragoza, Zaragoza, 256 p.

Bádenas. B., Aurell, M. (2001a): Proximal-distal facies relationships

and sedimentary processes in a storm dominated carbonate ramp (Kimmeridgian, northwest of the Iberian Ranges, Spain). *Sedimentary Geology* 139, 319-340. doi:10.1016/S0037-0738(00)00151-2.

Bádenas. B., Aurell. M. (2001b): Kimmeridgian palaeogeography and basin evolution of northeastern Iberia. *Palaeogeography, Palaeoclimatology, Palaeoecology* 168, 291-310. doi: 10.1016/S0031-0182(01)00204-8.

Bádenas, B., Aurell, M. (2004): Secuencias de alto orden en una rampa carbonatada dominada por las tormentas (Kimmeridgiense superior, Cordillera Ibérica septentrional). *Geo-Temas* 6, 35-38.

Bádenas, B., Aurell, M. (2010): Facies models of a shallow-water carbonate ramp based on distribution of non-skeletal grains (Kimmeridgian, Spain). *Facies* 56, 89–110. doi: 10.1007/s10347-009-0199-z.

Bádenas, B., Aurell, M., Meléndez, A. (1993): Características sedimentológicas, zonación y evolución de una rampa carbonatada dominada por tormentas (Kimmeridgiense, Cordillera Ibérica Septentrional). *Revista de la Sociedad Geológica de España* 6, 57-75.

Bádenas, B., Salas, R., Aurell, M. (2004): Three orders of regional sea-level changes control facies and stacking patterns of shallow platform carbonates in the Maestrat Basin (Tithonian-Berriasian, NE Spain). *International Journal of Earth Sciences* 93, 144-16. doi: 10.1007/s00531-003-0367-2.

Bathurst, R. G. C. (1975): *Carbonate Sediments and Their Diagenesis*. Developments in Sedimentology 12. Elsevier, Amsterdam, 658 p.

Bassoullet, J-P. (1997): Les Grands Foraminifères. In: E. Cariou and P. Hantzperque (coords.), Biostratigraphie du Jurassique ouest-européen et méditerranéen, *Bulletin Centre Recherche Elf Exploration-Production*, Mémoire 17, Pau, pp. 293-304.

Bhattacharya, J. P. (2006): Deltas. In: H. Posamentier and R. G. Walker (eds.), *Facies Models Revisited*, SEPM Special Publication 84, SEMP, Tulsa, pp. 237-292. DOI: 10.2110/pec.06.84.0237

Bhattacharya, J. P. (2010): Deltas. In: N. P. James and R. W. Dalrymple (eds.), *Facies Models 4*, Geological Association of Canada, Newfoundland pp. 233-264.

Calder, J. H., Gibling, M. R., Scott, A. C., Davies, S. J., Hebert, B. L. (2006): A fossil lycopsid forest succession in the classic Joggins section of Nova Scotia: paleoecology of a disturbance-prone Pennsylvanian wetland. In: S. F. Greb and W. A. DiMichele (eds.), *Wetlands through Time*. Geological Society of America, Special Papers 399, Boulder, pp. 169-195. doi:10.1130/2006.2399(09)

Canérot, J. (1974): *Reserches geologiques aux confins des chaines iberique et catalane (Espagne)*. Trabajos de Tesis, serie 5, número 4, Tolouse, 517 p. DUDA

Caron, V., Nelson, C. S., Kamp, P. J. J. (2005): Sequence stratigraphic context of syndepositional diagenesis in cool-water shelf carbonates: Pliocene limestones, New Zealand. *Journal of Sedimentary Research* 47, 231-250. doi:10.2110/jsr.2005.018

Campos-Soto, S., Benito, M. I., Mas, R., Quijada, I. E., Suarez-Gonzalez, P. (2015): Between tides, winds and rivers: deciphering challenging sandstone bodies in a multifaceted coastal system (Late Jurassic-Early Cretaceous, South Iberian Basin, SE Spain). *9th International Conference on Tidal Sedimentology*, Puerto Madryn, p. 46-49.

Clemmensen, L. B., Kenneth, P., Murray, A., Heinemeiers, J. (2001): Sedimentology, stratigraphy and landscape evolution of a Holocene coastal dune system, Lodbjerg, NW Jutland, Denmark. *Sedimentology* 48, 3-27. doi: 10.1111/j.1365-3091.2001.00345.x

Cobos, A., Royo-Torres, R., Luque, L., Alcalá, L., Mampel, L. (2010): An Iberian stegosaurs Paradise: The Villar del Arzobispo Formation. *Palaeogeography, Palaeoclimatology, Palaeoecology* 293, 223–236. doi:10.1016/j.palaeo.2010.05.024.

Daetwyler, C. C., Kidwell, A. L. (1959): The Gulf of Batabano, a modern carbonate basin. *Fifth World Petroleum Congress: proceedings*, New York, p. 1.

Dahanayake, K. (1977): Classification of oncoids from the Upper Juras-

sic carbonates of the French Jura. *Sedimentary Geology* 18, 337-353. doi: 10.1016/0037-0738(77)90058-6.

Dalrymple, R. W. (2010): Tidal Depositional Systems. In: N. P. James and R. W. Dalrymple (eds.), *Facies Models 4*, Geological Association of Canada, Newfoundland pp. 201-232.

Díaz, M., Yébenes, A. (1987): La sedimentación litoral y continental durante el Cretácico inferior. Sinclinal de Galve, Teruel. *Estudios geológicos* 43(Extra), 3-21. doi: 10.3989/egeol.8743Extra623.

Diedrich, C., Caldwell, M.W., Gingras, M. (2011): High-resolution stratigraphy and palaeoenvironments of the intertidal flats to lagoons of the Cenomanian (Upper Cretaceous) of Hvar Island, Croatia, on the Adriatic Carbonate Platform. *Carbonates Evaporites* 26, 381-399. doi:10.1007/s13146-011-0073-2.

Dunham, R.J. (1962): Classification of carbonate rocks according to depositional texture. In: W.E. Ham (ed.), *Classification of Carbonate Rocks*. Memoir 1, AAPG, Tulsa, Oklahoma, pp. 108- 121.

Enos, P. (1983): Shelf. In: P.A. Scholle, D.G. Bebout and C.H. Moore (eds.), *Carbonate depositional environments*. Memoir 33, AAPG, Tulsa, Oklahoma, pp. 267-296.

Flügel, E. (1982): Microfacies Analysis of Limestones. Springer-Verlag, Berlin, 633 p.

Flügel, E. (2010): *Microfacies of Carbonate Rocks: Analysis, Interpretation and Application*. Springer-Verlag, Berlin, Heidelberg, 984 p. doi: 10.1007/10.1007/978-3-642-03796-2.

Freytet, P., Plaziat, J. C. (1982): *Continental carbonate sedimentation and pedogenesis: Late Cretaceous and Early Tertiary of Southern France*. Contributions to Sedimentology 12, E. Schweizerbart´sche Verlagsbuchhandlun (Nägele u. Obermiller), Stuttgart, 213 p.

Fryberger, S. G., Krystinik, L. F., Schenk, C. J. (1990): Tidally flooded back-barrier dunefield, Guerrero Negro area, Baja California, Mexico. *Sedimentology* 37, 23-43. doi: 10.1111/j.1365-3091.1990.tb01981.x

Gómez, J.J. (1979): *El Jurasico en facies carbonatadas del Sector Levantino de la Cordillera Ibérica*. Seminarios de Estratigrafía, Serie Monografías 4, Madrid, 683 p.

Gómez, J.J., Goy, A. (1979): Las unidades litoestratigráficas del Jurasico medio y superior, en facies carbonatadas del Sector Levantino de la Cordillera Ibérica. *Estudios Geológicos* 35, 569- 598.

Gradstein, F.G., Ogg, J.G., Schmitz, M.D., Ogg, G.M. (2012): *The Geologic Time Scale*. Elsevier, Boston, 114 pp. doi: 10.1016/B978-0-444-59425-9.00004-4

Halley, R. B., Harris, P. M., Hine, A. C. (1983): Bank Margin. In: P.A. Scholle, D.G. Bebout and C.H. Moore (eds.), *Carbonate depositional environments*. Memoir 33, AAPG, Tulsa, Oklahoma, pp. 463-506.

Hammer, Ø., Harper, D. A. T., Ryan, P. D. (2001): Past: Paleontological Statistics Software Package for Education and Data Analysis. *Palaeontologia electronica* 4, 1-9.

Harris, P. M., Purkis, S. J., Ellis, J. Swart, P. K., Reijmer, J. J. G. (2015): Mapping bathymetry and depositional facies on Great Bahama Bank. *Sedimentology* 62, 566-589. doi:10.1111/sed.12159

Hoskins, C. W. (1964): Molluscan biofacies in calcareous sediments, Gulf of Batabano, Cuba. *Bulletin of the American Association of Petroleum Geologists* 48, 1690-1704. doi: 10.1306/BC7437B3-16BE-11D7-8645000102C1865D

Hottinger, L. (1967): Foraminiferes imperforés du Mésozoique marocain, *Notes et Mémoires du Service Géologique du Maroc* 209, 168 p.

Hunter, R. E., Richmond, B. M., Alpha, T. R. (1983): Storm-controlled oblique dunes of Oregon Coast. *Geological Society of American Bulletin* 94, 1450-1465.

Ipas, J., Aurell, M., Bádenas, B. (2004): Ambientes sedimentarios y secuencias en la Fm. Higueruelas (Jurásico Superior) en la Cordillera Ibérica Septentrional. *Geogaceta* 35, 7-10.

James, N. P. (1977): Facies Models 8. Shallowing-Upward Sequences in Carbonates. Geoscience Canada 4, 126-136.

Kaczmareck, S. E., Hicks, M. K., Fullmer, S. M., Steffen, K. L., Bach-

tel., S.L. (2010): Mapping facies distributions on modern carbonate platforms through integration of multispectral Landsat data, statistics-based unsupervised classifications, and surface sediment data. *AAPG Bulletin* 94, 1581-1606. doi: 10.1306/04061009175.

Kocurek, G. (1981): Significance of interdunes deposits and bounding surfaces in aeolian dune sands. *Sedimentology* 28, 753-780. doi: 10.1111/j.1365-3091.1981.tb01941.x

Langford, R. P. (1989): Fluvial-aeolian interactions: Part I, modern systems. *Sedimentology* 36, 1023-1035. doi: 10.1111/j.1365-3091.1989.tb01540.x

Langford, R.P., Chan, M.A. (1989): Fluvial-aeolian interactions: Part II, ancient systems. *Sedimentology* 36, 1037-1051. doi: 10.1111/j.1365-3091.1989.tb01540.x

Loeblich, A. R., Tappan, H. (1987): *Foraminiferal Genera and their Classification. Van Nostrand Rienhold Company*, New York, 2 vol., 970p.

Luque, L., Cobos, A., Royo-Torres, R., Espílez, E., Alcalá, L. (2005): Caracterización de los depósitos sedimentarios con dinosaurios de Riodeva (Teruel). *Geogaceta* 38, 27-30.

Martin-Closas, C., Serra-Kiel, J. (1991): Evolutionary Patterns of Clavatoraceae (Charophyta) in the mesogean basins analyzed according to environmental change during Malm and Lower Cretaceous. *Historical Biology* 5, 291-307. doi:10.1080/10292389109380408.

Martinius, A. W., Van den Berg, J. H. (2011): *Atlas of sedimentary structures in estuarine and tidally-influenced river deposits of the Rhine-Meuse-Scheldt system: Their application to the interpretation of analogous outcrop and subsurface depositional systems.* EAGE Publications, Houten, 298 pp.

Mas, R. (1981): *El Cretácico inferior de la región Noroccidental de la provincia de Valencia. Seminarios de Estratigrafía*, Serie Monografías 8, Madrid, 476 p.

Mas, R., Alonso, A. (1981): *Trabajo estratigráfico, sedimentológico y paleogeográfico de las facies Purbeck, Weald y Utrillas en el sector suroriental de la Cordillera Ibérica*. Hoja geológicas num. 55 (Lliria) y 43 (Valencia) del Mapa Geológico de España E. 1:200.000. Segunda serie, IGME, Madrid, 120 p. Unpublished.

Mas, R., Alonso, A., Meléndez, N. (1982): El Cretácico basal "Weald" de la Cordillera Ibérica Suroccidental (NW de la provincia de Valencia y E de la de Cuenca). *Cuadernos de Geología Ibérica* 8, 309-335.

Mas, R., Alonso, A., Meléndez, N. (1984): La formación Villar del Arzobispo: un ejemplo de llanuras de mareas siliciclásticas asociadas a plataformas carbonatadas. Jurasico terminal. (NW de Valencia y E de Cuenca). *Publicaciones de Geología* 20, 175-188.

Mas, R., García, A., Salas, R., Meléndez, A., Alonso, A., Aurell, M., Bádenas, B., Benito, M.I., Carenas, J.F., García-Hidalgo, J., Gil, J., Segura, M. (2004): Segunda fase de rifting: Jurásico Superior-Cretácico Inferior. In: J.A. Vera (ed.), *Geología de España*, SGE-IGME, Madrid, pp. 503-510.

Marsaglia, K.M., DeVries, G. (1983): The paleogeography of Paleozoic and Mesozoic storm depositional systems. *The Journal of Geology* 91, 117-142. doi: 10.1086/628752

Maync, W. (1960): Biocaractères et analise morphométrique des espèces jurassiques du genre Pseudocyclammina (Foaminifères): Peudocyclammina jaccardi (Schrodt). *Revue Micropaléontologie* 3, 103-118.

Mountney, N. P. (2006): Aeolian Facies Models. In: H. Posamentier and R. G. Walker (eds.), *Facies Models Revisited*, SEPM Special Publication 84, SEMP, Tulsa, pp. 19-83. DOI: 10.2110/pec.06.84.0019

Mutti, E., Davoli, G., Tinterri, R., Zavala, R. (1996): The Importance of Ancient Fluvio-Deltaic Systems Dominated by Catastrophic Flooding in Tectonically Active Basins. *Memorie di Scienze Geologiche* 8, 233-291.

Nio, S. D.,Yang, C. S. (1991): Diagnostic attributes of clastic tidal deposits: a review. In: D. G. Smith, G. E. Reinson, B. A. Zaitlin and R.A. Rahmani (eds.), *Clasitc Tidal Sedimentology*. Canadian Society of Petroleum Geologists Mem., 16, Calgary, 3-28.

Pereda, X., Ruiz-Omeñaca, J. I., Company, J. (2009): Primera descripción de restos esqueléticos de dinosaurio ornitópodo en la Formación Villar del Arzobispo (tránsito Jurásico-Cretácico): yacimiento de Cerrito del Olmo (Alpuente, Valencia). *Geogaceta* 47, 13-16.

Pérez-García, A., Sánchez, B., Ortega, F. (2009): Aportaciones sobre José Royo y Gómez al conocimiento sobre los dinosaurios de España. *Paleolusitana* 1, 339-364.

Pontén, A., Plink-Björklund, P. (2009): Regressive to transgressive transits reflected in tidal bars, Middle Devonian Baltic Basin. *Sedimentary Geology* 218, 48-60. doi: 10.1016/j.sedgeo.2009.04.003.

Purdy, E. G. (1963): Recent Calcium Carbonate Facies of The Great Bahama Bank 2. Sedimentary Facies. *The Journal of Geology* 71, 472-497. doi:10.1086/626920.

Reijmer, J. J. G., Swart, P.K., Bauch, T., Otto, R., Reuning, L., Roth, S., Zechel, S. (2009): A re-evaluation of facies on Great Bahama Bank I: new facies maps of western Great Bahama Bank. In: P. K. Swart, G. P. Eberli, J. A. McKenzie, I. Jarvis and T. Stevens (eds.), *Perspectives in Carbonate Geology: A Tribute to the Career of Robert Nathan Ginsburg*. John Wiley & Sons, Ltd, Chichester, West Sussex, United Kingdom, pp. 29-46. doi: 10.1002/9781444312065.ch3.

Reineck, H-E., Wunderlich, F. (1968): Classification and origin of flaser and lenticular bedding. *Sedimentology* 11, 99-104.

Ricci-Lucchi, F. (1975): Depositional cycles in two turbidite formations of northern Apennines (Italy). *Journal of Sedimentary Petrology* 45, 3-43.

Rodríguez-López, J. P., Meléndez, N., De Boer, P. L., Soria, A. R. (2008): Aeolian sand sea development along the mid-Cretaceous western Tethyan margin (Spain): erg sedimentology and palaeoclimate implications. *Sedimentology* 55, 1253-1292. doi: 10.1111/j.1365-3091.2007.00945.x

Rodríguez-López, J. P., Meléndez, N., De Boer, P. L., Soria, A. R. (2012): Controls on marine-erg margin cycle variability: aeolian-marine interaction in the mid-Cretaceous Iberian Desert System, Spain. *Sedimentology* 59, 466-501. doi: 10.1111/j.1365-3091.2011.01261.x

Royo-Torres, R., Cobos, A., Luque, L., Aberasturi, A., Espílez, E., Fierro, I., González, A., Mampel, L., Alcalá, L. (2009): High european sauropod dinosaur diversity during Jurassic-Cretaceous transition in Riodeva (Teruel, Spain). *Palaeontology* 52, 1009-1027. doi: 10.1111/j.1475-4983.2009.00898.x

Royo y Gómez, J. (1926a): Los vertebrados del Cretácico español de facies weáldica. *Boletín del Instituto Geológico y Minero de España* 47, 171-176.

Royo y Gómez, J. (1926b): Notas geológicas sobre la provincia de Valencia. *Boletín de la Real Sociedad Española de Historia Natural* 26, 66-87.

Royo y Gómez, J. (1927): Nuevos descubrimientos paleontológicos en la facies weáldica de Levante. *Boletín de la Real Sociedad Española de Historia Natural* 27, 113-115.

Rygel, M. C., Calder, J. H., Gibling, M. R., Gingras, M. K., Melrose, C. S. A. (2006): Tournaisian forested wetlands in the Horton Group of Atlantic Canada. In: S. F. Greb and W. A. DiMichele (eds.), *Wetlands through Time*. Geological Society of America, Special Papers 399, Boulder, pp. 103-126. doi:10.1130/2006.2399(05)

Salas, R. (1987): *El Malm i el Cretaci inferior entre el Massís de Garraf i la Serra D´Espada. Anàlisi de conca.* Tesis Doctoral, Universitat de Barcelona, Barcelona, 345p.

Salas, R., Guimerà, J., Mas, R., Martin-Closas, C., Melendez, A., Alonso, A. (2001): Evolution of the Mesozoic Central Iberian Rift System and its Cainozoic inversion (Iberian chain). In: W. Cavazza, A.H.F.R. Roberston, P. Ziegler (eds.), *Peri-Tethyan Rift/Wrech basins and Passive Margins.* Mem. Musee National Histoire Naturelle, Paris, pp. 145-185.

Sano, H., Onoue, T., Orchard, M. J., Martini, R. (2012): Early Triassic peritidal carbonate sedimentation on a Panthalassan seamount: the

Jesmond succession, Cache Creek Terrane, British Columbia, Canada. *Facies* 58, 113-130. doi: 10.1007/s10347-011-0270-4

Santisteban, C., Gaete, R., Galobart, A., Suñer, M. (2002): Rastros de dinosaurios en el Jurasico terminal (Facies Purbeck) de Corcolilla (Los Serranos, Valencia). *Dinosaurios y otros reptiles mesozoicos en España*, 33-40.

Santisteban, C., Suner, M., Vila, B. (2008): El yacimiento de icnitas de dinosaurios de Canada Paris, Alpuente, Valencia. *Actas de las IV Jornadas Internacionales sobre Paleontología de Dinosaurios y su Entorno*, Salas de los Infantes, Burgos, p. 301.

Sasser, C. E., Gosselink, J. G., Holm, G. O., Visser, J. M. (2009): Tidal freshwater wetlands of the Mississippi River deltas. In: A. Barendregt, D. Whigham and A. Baldwin (eds*.), Tidal Freshwater Wetlands*. Backhuys Publishers, Leiden, pp. 167-178.

Suarez-Gonzalez, P. Quijada, I. E., Benito, M. I., Mas, R. (2015): Sedimentology of Ancient Coastal Wetlands: Insights From A Cretaceous Multifaceted Depositional System. *Journal of Sedimentary Research* 85, 95-117. doi:10.2110/jsr.2015.07.

Suñer, M., Poza, B., Vila, B., Santos-Cubedo, A. (2008): Síntesis del registro fósil de dinosaurios en el Este de la Península Ibérica. *Palaeontologica Nova* 8, 397-420.

Tripaldi, A., Limarino, C. O. (2008): Ambientes de interacción eólica-fluvial en valles intermontanos: ejemplos actuales y antiguos. *Latin American Journal of Sedimentology and Basin Analysis* 15, 43-66.

Trullenque. (1915): Sesión de Valencia. *Boletín de la Real Sociedad Española de Historia Natural* 15, 103-104.

Tucker, M., Wright, V.P. (1990): *Carbonate sedimentology*. Blackwell, Oxford, 482 p. doi: 10.1002/9781444314175

Turner, B. R., Tester, G., N. (2006): The Table Rock Sandstone: A fluvial, friction-dominated lobate mouth bar sandbody in the Westfalian B Coal Measures, NE England. *Sedimentary Geology* 190, 97-119. doi:10.1016/j.sedgeo.2006.05.007

Viallard, P. (1973): *Reserches sur le cycle alpin dans la Chaine ibérique sud-occidentale*. Tesis, Travaux du laboratorie de géologie mediterranéenne, Université Paul Sabatier, Tolouse, 445 p.

Vilas, L., Mas, R., García, A., Arias, C., Alonso, A., Meléndez, N., Rincón, R. (1982): Capítulo 8 Ibérica suroccidental. In: A. García (ed.), *El Cretácico de España*. Universidad Complutense, Madrid, pp. 457-514.

Wagner, C. W., Van der Togt, C. (1973): Holocene sediment types and their distribution in the southern Persian Gulf. In: B.H., Purser (ed.), *The Persian Gulf*: Springer-Verlag, New York, pp. 123–155.

Wilkinson, B. H., Drumond, C. N. (2004): Facies mosaic across the Persian Gulf and around Antigua-Stochastic and deterministic products of shallow-water sediment accumulation. *Journal of Sedimentary Research* 74, 513-526. doi: 10.1306/123103740513

Wilson, J.L. (1975): *Carbonate facies in geologic history*. Springer-Verlag, New York, 471 p.

Wolanski, E., Brinson, M. M., Cahoon, D. R., Perillo, G. M. E. (2009): Coastal Wetlands: a synthesis. In: G. M. E. Perillo, E. Wolanski, D. R. Cahoon and M. M. Brinson (eds.), *Coastal Wetlands. An integrated ecosystem approach*. Elsevier, Amsterdam, pp. 1-62.

Woodroffe, C. D., Davies, G. (2009): The morphology and development of tropical coastal wetlands. In: G. M. E. Perillo, E. Wolanski, D. R. Cahoon and M. M. Brinson (eds.), *Coastal Wetlands. An integrated ecosystem approach*. Elsevier, Amsterdam, pp. 65-88.

Wright, V.P., Wilson, C.L. (1984): A carbonate submarine-fan sequence from the Jurassic of Portugal. *Journal of Sedimentary Petrology* 54, 394-412. doi:10.1306/212F8427-2B24-11D7-8648000102C1865D.

Zhang, Q.-H., Ding, L., Cai, F.-L., Xu, X.-X., Zhang, L.Y., Xu, Q., Willems, H. (2011): Early Cretaceous Gangdese retroarc foreland basin evolution in the Selin Co basin, central Tibet: evidence from sedimentology and detrital zircon geochronology. *Geological Society Special Publications* 353, 27-44. doi: 10.1144/SP353.3.

Zuffa, G.G. (1980): Hybrid arenites: their composition and classification. *Journal of Sedimentary Research* 50, 21-29. doi: 10.1306/212F7950-2B24-11D7-8648000102C1865D